Arabidopsis *hydroperoxide lyase* gene: spatial temporal expression and the involvement of its metabolic products during *Arabidopsis-Pseudomonas* interaction

A dissertation submitted in partial fulfilment of the requirements for the degree of Doctor of Philosophy at Yamaguchi University

by

Cynthia Nyambura Mugo - Mwenda

MSc Yamaguchi University, 2012

BSc Kenyatta University, 2007

Supervisor: Professor Kenji Matsui

Yamaguchi University

September 2015

Acknowledgments

Prof. Matsui laboratory, thank you for your time, friendship, help, memorable experiences and good laughs.

I would like to thank my family for their treasured love, endless support and encouragement. At last, but not least, my best friend and husband Dickson Mwenda Kinyua, for his endless support and patience.

Dedication

This thesis is a dedication to my loving mother who passed away in the last semester of my

study.

12th September, 2014

Table of Contents

1   CHAPTER ONE

Spatial expression of the Arabidopsis *hydroperoxide lyase* gene is controlled differently from that of the *allene oxide synthase* gene

Abstract

The hydroperoxide lyase (HPL) pathway for six carbon (C6) volatiles and the allene oxide synthase (AOS) pathway for jasmonates (JAs) share the first part of the pathway. To avoid competition, a separate localization of HPL and AOS might be important. A fusion protein comprising Arabidopsis HPL and green fluorescent protein was transported into chloroplasts, where AOS was located. Arabidopsis harboring β-glucuronidase (GUS) gene downstream of Arabidopsis HPL promoter (pAtHPL::GUS) showed different GUS activity in floral organs compared with that from pAtAOS::GUS. With pAtHPL::GUS, wounding enhanced GUS activity at the periphery of cotyledons; while with pAtAOS::GUS, GUS activity was high in the vasculature. The distribution of the ability to form C6 volatiles correlated with the profile of HPL promoter activity; however, this ability unchanged after wounding. Inconsistency between the AOS promoter activity and JA levels was also evident. Thus, an additional factor should also control the ability to form C6 volatiles and JAs.

1.1 Introduction

Plants have evolved complex signaling pathways to ensure effective responses to biotic and abiotic challenges, as well as to developmental stimuli. The oxylipin pathway is one such pathway, which, upon activation by environmental and developmental inputs, induces the synthesis of a diverse group of bioactive compounds known as oxylipins (Feussner & Wasternack 2002; Howe & Schilmiller 2002). Oxylipin biosynthesis is initiated by lipoxygenases, leading to the oxygenation of polyunsaturated fatty acids, mainly linoleic and α-linolenic acids, to yield their 9- or 13-hydroperoxides (9-/13-hydroperoxyoctadecadienoic acid, and 9-/13-hydroperoxyoctadecatrienoic acid [9-/13-HPOT]; Chehab et al. 2006). These hydroperoxides are metabolized by a group of cytochrome P450 enzymes present in different branch pathways, to generate the oxylipins (Feussner & Wasternack 2002). Among the oxylipin branch pathways, the hydroperoxide lyase (HPL) and the allene oxide synthase (AOS) are considered the two major plant stress response pathways. AOS and HPL are related cytochrome P450s, designated CYP74A and 74B, respectively (Song & Brash 1991; Shibata et al. 1995a, 1995b; Nelson 1999), which metabolize a common fatty acid hydroperoxide substrate (13-HPOT) to different classes of bioactive oxylipins.

13-HPL (CYP74B) cleaves 13-HPOT at the C12-C13 bond to produce two carbonyl compounds: (Z)-3-hexenal and 12-oxo-(Z)-9-dodecenoic acid (Grechkin and Hamberg 2004). A nicotinamide adenine dinucleotide phosphate dependent reductase reduces (Z)-3-hexenal to (Z)-3-hexen-1-ol (Matsui et al. 2012), which can be further converted to (Z)-3-hexen-1-yl acetate by acetylcoenzyme A: (Z)-3-hexen-1-ol acetyltransferase (D'Auria et al. 2007). In some plants, (Z)-3-hexenal is converted to (E)-2-hexenal spontaneously or enzymatically (Noordermeer et al. 1999; Matsui 2006; D'Auria et al. 2007). These C6-aldehydes, alcohols, and their corresponding

esters of the HPL pathway are collectively known as green leaf volatiles (GLVs; Matsui 2006; Nyambura et al. 2011). Insecticidal, fungicidal, and bactericidal activities have been reported for (Z)-3-hexenal and its related aldehydes (Hamilton-Kemp et al. 1992; Croft et al. 1993; Hammond et al. 2000; Vancanneyt et al. 2001; Nakamura and Hatanaka 2002; Hubert et al. 2008; Kishimoto et al. 2008). They also function as airborne infochemicals in specific plant herbivore, plant–carnivore, and plant–plant relationships (Arimura et al. 2009; Sugimoto et al. 2014).

AOS (CYP74A) transforms 13-HPOT to epoxy octadecatrienoic acid (EOT), which is converted spontaneously into α- and γ-ketols, and 12-oxophytodienoic acid (OPDA). In the presence of allene oxide cyclase, EOT is specifically converted to OPDA, and then, to jasmonic acid (JA) after several enzymatic reaction steps (Froehlich et al. 2001; Mosblech et al. 2009). JA and related cyclopentanone products of the AOS pathway (jasmonates, JAs) are essential signals in the defense against mechanical wounding and attacks by herbivores and necrotrophic pathogens; they are also involved in developmental processes (Creelman & Mullet 1997; Staswick & Lehman 1999; Brioudes et al. 2009; Glauser et al. 2009; Hause et al. 2009; Erb et al. 2012).

JAs from the AOS pathway and GLVs from the HPL pathway exert distinct bioactivities and functions; therefore, their formation should be finely tuned. Given that HPL and AOS show similar substrate specificities (Taurino et al. 2013), it is assumed each pathway is fine-tuned to avoid competition between HPL and AOS for the same substrate (13-HPOT).

The temporal expression profiles of *AOS* and *HPL* show a partial overlap. Wound-inducible increases in *HPL* and *AOS* transcript levels have been documented in Arabidopsis (Bate et al. 1998; Laudert & Weiler 1998; Matsui et al. 1999; Kubigsteltig et al. 1999; Howe et

4

al. 2000). Exogenous application of methyl jasmonates (MeJA) increases both *HPL* and *AOS* transcript levels (Avdiushko et al. 1995; Kohlmann et al. 1999; Matsui et al. 1999; Sivasankar et al. 2000; Ziegler et al. 2001).

The subcellular localization of AOS and HPL should also be considered in understanding to what degree these two enzymes would compete. AT_Chloro (http://www.grenoble.prabi.fr/at_chloro/), a database dedicated to the chloroplast proteome from Arabidopsis, shows that *Arabidopsis thaliana AOS* (*AtAOS*) is targeted to the chloroplast envelope. Additionally, a link between *AtAOS* accumulation and chloroplast rhomboid proteases, both of which reside in the chloroplast envelope, has been reported (Knopf et al. 2012). Most 13-HPLs (CYP74B) examined to date have an N-terminal extension that is predicted to be a chloroplast transit peptide, according to a prediction method such as ChloroP (http://www.cbs.dtu.dk/services/ChloroP/). Froehlich et al. (2001) showed that tomato HPL and AOS are targeted to the outer and inner membranes of the chloroplast envelope, respectively. Rice HPL3 (OsHPL3), which has the shortest extension of its N-terminal among the three HPLs, was transported to chloroplasts when a fusion protein of the transit peptide of OsHPL3 with green fluorescent protein (GFP) was expressed in Arabidopsis leaves (Savchenko et al. 2014). However, localization of HPL in Arabidopsis has not been reported. There is no entry for HPL in AT_Chloro because the proteome analysis was carried out with Col-0, a natural *hpl* loss-of-function mutant (Duan et al. 2005).

Cellular and tissue distribution of expression of HPL and AOS should be taken into account to evaluate their competition as well as their distinct physiological functions. We addressed this issue using reporter assays with GFP and β-glucuronidase (GUS). We also examined the metabolic levels of GLVs and JAs. First, we examined subcellular and tissue

localizations of HPL and C6-aldehydes. Thereafter, we examined responses of HPL promoter and AOS promoter against mechanical wounding with the GUS reporter system. We also examined distribution of GLVs and JAs in leaf tissues upon mechanical wounding. The differences in the spatial and temporal expression patterns of *HPL* and *AOS* observed in this study provide an additional insight into how these two genes are regulated to avoid substrate competition during oxylipin synthesis.

1.2   Materials and methods

1.2.1   Plant material and growth conditions

Wild-type ecotypes (Col-0 and *No-0*) of *Arabidopsis thaliana*, and transgenic lines *pAtAOS::GUS* (C24) (Kubigsteltig et al. 1999) (kindly provided by Dr. Ines Kubigsteltig, Ruhr-Universität, Bochum, Germany), and *pVSP::GUS* (*Col-gl1*) (Xie et al. 1998) (kindly provided by Prof. John G. Turner, University of East Anglia, UK) were grown sterilely on B5 medium plates at 22 °C with light from fluorescent lights (14 h light/10 h dark). Seedlings grown for 8 days were used for GUS staining. For the analysis of C6- volatiles and phytohormones in dissected leaves, 4-week-old Arabidopsis wild-type ecotype *Nössen-0* (*No-0*) grown in soil (Vermiculite and Metro-mix) at 22 °C and 70% relative humidity with light from fluorescent lights (14 h light/10 h dark) was used.

1.2.2   Construction of the reporter systems: pAtHPL::GFP and pAtHPL::GUS

Genomic DNA was purified from Col-0 leaves, and the DNA encoding the N-terminal half (from Met1 to Asn275) of AtHPL (At4g15440) was PCR-amplified with primers (5′–

GTCGACATGTTGTTGAGAACGATGGCG–3′ and 5′–CCATGGGTTCTCGTCGATGAAAT–

3′). The resultant amplicon was inserted into *Sal* I and *Nco* I digested 35Ω-sGFP (S65T) (Chiu et

al. 1996) (kindly provided by Dr. Y. Niwa, University of Shizuoka, Shizuoka, Japan). The

plasmid was propagated in *Escherichia coli* and then transiently introduced into Arabidopsis

leaflet using particle bombardment.

To prepare the GUS construct, the promoter region (−2120 to +33 nucleotides relative to

the translation start codon) of AtHPL (At4g15440) was PCR amplified with primers

(5′CCCAAGCTTCACATTGCTCTGAACTGAATCGCCTAG-3′ and 5′

CGGGATCCGCGGGGAAGTCGCCGCCATCGTTC-3′), and the resultant amplicon was

inserted into *BamH*I and *Hind*III digested pBI101.3. The gene was introduced into Col-0

Arabidopsis through the floral dip method using *Agrobacterium tumefaciens* (LBA4404) as a

transient host (Weigel & Glazerbrook 2002). Transgenic plants (*pAtHPL::GUS*) were selected by

kanamycin resistance and PCR confirmation of the transgene. Homozygotes of the T5–T7

generations were used for the GUS monitoring. Homozygous *pAtHPL::GUS* plants were crossed

with *coi1* (Xie et al. 1998) (kindly provided by Prof. John G. Turner, University of East Anglia,

UK) or *dad1* (Ishiguro et al., 2001). Homozygotes of *coi1* confirmed its male sterility among the

progeny of *coi1* heterozygotes. Homozygotes of *dad1* were obtained by rescuing its male sterility

by dipping young buds into 0.5 mM MeJA suspended with 0.05% (w/v) Tween 20.

1.2.3 GFP reporter assays

AtHPL::GFP was introduced into leaf epidermal cells of Arabidopsis (Col-0) by particle

bombardment, as previously described (Tanaka et al. 2013), in which the helium pressure was 4

kgf cm^{-2} under a vacuum of 80 kPa. Following bombardment, the agar plate was filled with

water to prevent desiccation. After incubation overnight at 22 °C in the dark, leaves were viewed with a TCS SP5 confocal laser scanning microscopy (Leica Microsystems, Wetzlar, Germany) using an HCX PL APO CS 20.0 × 0.70 WATER UV objective lens. The GFP and chlorophylls were exited by the argon laser line (488 nm). The fluorescence of GFP was detected at 500–530 nm, whereas chlorophyll autofluorescence was detected at 770–800 nm. Images were processed with Photoshop CS6 (Adobe Systems, San Jose, CA, USA).

1.2.4 GUS activity assays

Histochemical staining of plant tissues for GUS activity was performed according to published protocols (Weigel & Glazerbrook 2002). Briefly, samples were placed in substrate solution (50 mM sodium phosphate pH 7.2, 2 mM potassium ferrocyanide, 2 mM potassium ferricyanide, and 0.2% Triton X-100 containing 1 mM 5-bromo-4-chloro-3-indoyl-β-D-glucoronide), vacuum infiltrated for 20 min, and then incubated at 37 °C for 18 h. Subsequently, the samples were subjected to a series of 20, 35, and 50% ethanol, and then fixed in formalin-ehtanol-acetic acid solution (FAA) and finally transferred to 70% ethanol to remove the chlorophyll. Mechanical wounding was accomplished by applying pressure for 5 s using forceps on one side of the cotyledon of 8-day-old seedlings. The mid-vein was carefully left intact. Control samples were not wounded.

1.2.5 Determination of JAs

To determine the amounts of JAs in the mid-veins and the remaining leaf lamina, fully developed rosette leaves of 4-week-old *A. thaliana* ecotype *No-0* plants were wounded by applying pressure with forceps three times on one side of the leaf lamina (corresponding to ca.

30% wound area on the treated side). Samples pooled from at least three different plants were taken from unwounded (control) and wounded tissue at different time points after wounding. The leaf was dissected into three parts using a sharp razor blade. Approximately 50 mg of tissue samples from the mid-vein and the opposite unwounded leaf lamina were collected within 30 s in disruptor tubes containing two glass beads (2 mm i.d.) and two steel beads (3 mm i.d.), flash-frozen in liquid nitrogen, and stored at −80 °C until use. One millilitre of ethyl acetate spiked with 20 ng of D_2JA (Sigma-Aldrich, St. Luis, MO, USA), used as the internal standard, was added to each sample, which was then completely homogenized on a MicroSmash homogenizer (MS-100R; Tomy Digital Biology Co. Tokyo, Japan). After centrifugation at $12,000 \times g$ for 10 min at 4 °C, supernatants were transferred to fresh 2 mL microtubes. Each pellet was re-extracted with 0.5 mL of ethyl acetate and centrifuged; supernatants were combined and then evaporated to dryness on a vacuum concentrator. The residue was resuspended in 0.5 mL of 70% methanol (v/v) and centrifuged to clarify the phases. The supernatants were pipetted into glass vials and then analysed by liquid chromatography tandem mass spectrometry (LC-MS/MS).

JA and JA-Ile were analysed by LC-MS/MS (3200 Q-TRAP LC/MS/MS System (AB Sciex, Framingham, MA, USA) equipped with Prominence UFLC (Shimadzu, Kyoto, Japan). At a flow rate of 0.2 mL min^{-1}, 2 μL of each sample was injected onto a Mightysil RP18 column (5 μm, 150 × 2 mm). A mobile phase composed of solvent A (water/acetonitrile/formic acid (90:10:0.1, v/v) and solvent B (acetonitrile/water/formic acid (95:5:0.1, v/v) was used in a gradient mode for separation. The solvent gradient used was 100% A to 100% B over 20 min, hold at 100% B for 5 min and then the solvent returned to 100% A for 15 min equilibration before the next injection. The MS was used in negative ion mode and ions were detected using multiple reaction monitoring. The parent ions, daughter ions and parameters used for their

detection are listed in **Table 1-1**. Quantification was made based on the internal standard added and standard curves.

1.2.6 Determination of GLVs

For the determination of C6 volatiles, fully developed rosette leaves of 4-week-old *A. thaliana* ecotype *No-0* plant were mechanically wounded and dissected as described above. Approximately 50 mg of the dissected mid-veins and remaining leaf lamina were collected separately in a glass vial (22 mL; Perkin Elmer, Waltham, MA, USA) and immediately stored at −80 °C until use. Samples were thawed for 10 min in a water bath set at 25 °C, and then, 1 mL of saturated $CaCl_2$ solution was added to halt any enzyme reactions. An SPME fibre (50/30 μm DVB/Carboxen/PDMS Stable Flex; Supelco, Bellefonte, PA, USA) was exposed to the headspace of the vial for 30 min at 25 °C. The fibre was inserted into the insertion port of a gas chromatography-mass spectrometry (GC-MS) apparatus (QP-2010 Plus; Shimadzu, Kyoto, Japan) equipped with a stabiliwax column (30 m × 0.25 mm i.d. × 0.25 μm film thickness) (Restek, Bellefonte, PA, USA). The column temperature was programmed as follows: 40 °C for 5 min, increasing by 5 °C min^{-1} to 200 °C for 2 min. The carrier gas (He) was delivered at a flow rate of 1.54 mL min^{-1}. The glass insert was an SPME Sleeve (Supelco). The fibre was held in the injection port for 10 min at 240 °C to fully remove any compounds from the matrix. Splitless injection with a sampling time of 1 min was used. The temperatures of the ion source and interface were 200 and 240 °C, respectively. The mass detector was operated in the electron impact mode, with ionisation energy of 70 eV. To identify each compound, retention indices and MS profiles of corresponding authentic compounds were used. The quantities of GLVs were

determined from the peak areas, based on a calibration curve constructed with known amounts of GLVs suspended in 1 mL saturated $CaCl_2$ solution.

1.3 Results

1.3.1 Determining the subcellular localization of AtHPL using a GFP reporter assay

A ChloroP prediction suggested that the N-terminal sequence consisting of 34 amino acids of AtHPL was a transit peptide for chloroplast targeting. We fused the complementary DNA (cDNA) sequences encoding the N-terminal half of AtHPL to the cDNA encoding GFP. The fusion protein was expressed transiently under the control of cauliflower mosaic virus 35S promoter in Arabidopsis leaves using the particle gun bombardment technique (Tanaka et al. 2013). The fluorescence signals of AtHPL::GFP fusions were found in chloroplasts, as identified by imaging of the autofluorescence of chlorophyll (**Figure 1-1**). The image was almost identical to that obtained with GFP fused to the transit peptide derived from the Arabidopsis ribulose-1,5-biphosphate carboxylase small subunit (Chiu et al. 1996), while GFP without the additional peptide was located in the cytoplasm and nuclei (Chiu et al. 1996). These results showed that AtHPL is localized to the chloroplasts.

	GFP	Chlorophyll	Merge
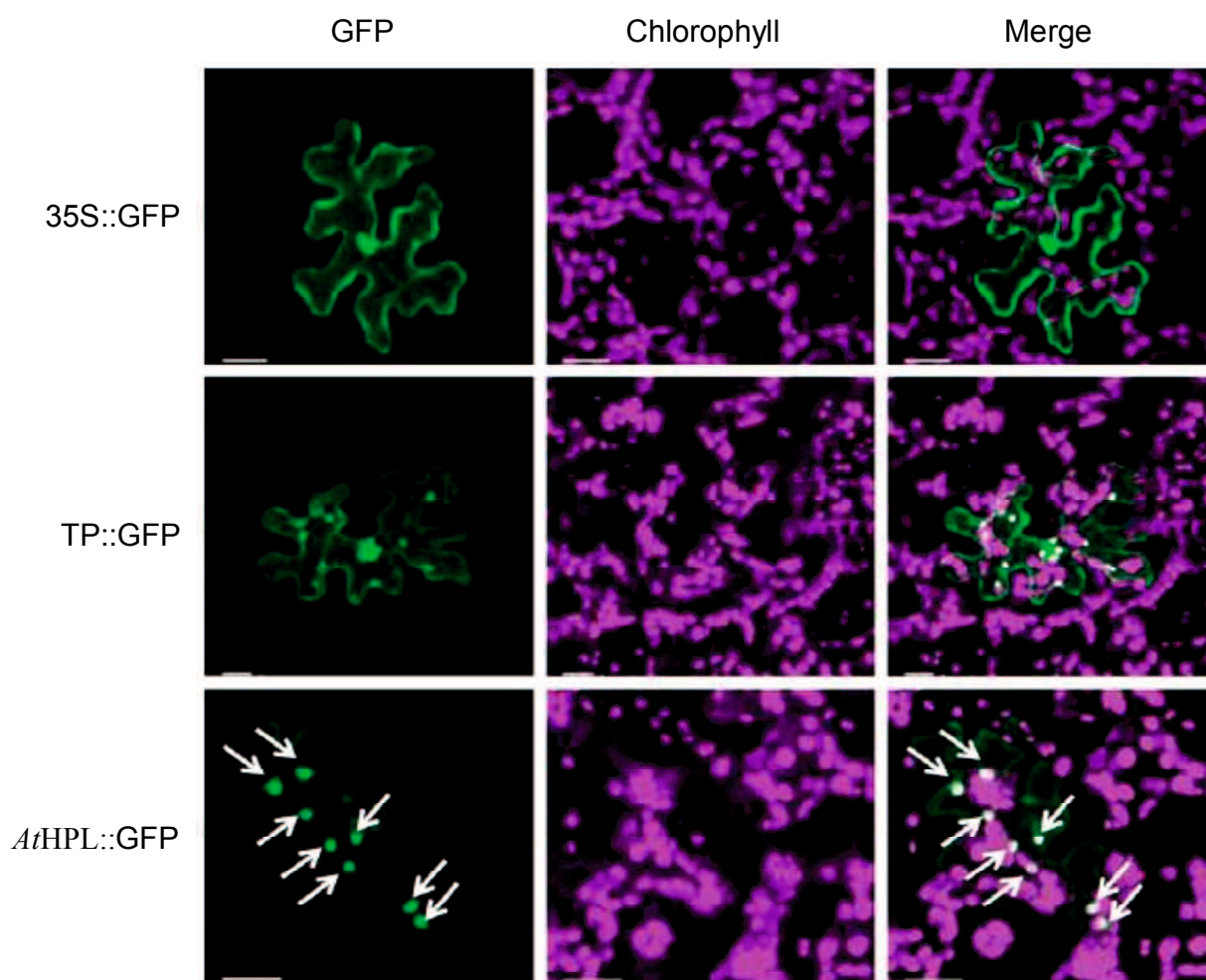
Figure 1-1. Subcellular localization of the AtHPL::GFP fusion protein under the control of the CaMV 35S promoter. 35S::GFP, 35S::TP::GFP (positive controls) and 35S::AtHPL::GFP fusion proteins were expressed transiently in Arabidopsis leaves using the particle gun bombardment technique. Expression was monitored using confocal microscopy. AtHPL::GFP was expressed in the chloroplasts on the epidermal surface of *A. thaliana* leaves, as observed in the merged images. White arrows mark chloroplasts expressing *At*HPL::GFP. Magenta depicts autofluorescence of chlorophyll. Scale bar is 20 μm.

1.3.2 *GUS reporter assay to determine the expression profile of AtHPL*

We fused the promoter region (2152 bp of the 5′ upstream sequence) of the *AtHPL* gene (*pAtHPL*) to the GUS gene and transformed Arabidopsis (Col-0) with the fusion gene. When the

transgenic plants were grown under normal growth conditions, we noticed significant GUS expression in the inflorescence (**Figure 1-2 A, B, and E**). This agrees with the results of northern blot analysis indicating that the transcript of *AtHPL* was abundant in inflorescences, flowers, and siliques (Bate et al. 1998; Matsui et al. 1999). High GUS activity was evident in carpels, filaments, peduncles, and sepals in open flowers; however, anthers, stigmas, and petals showed little activity. The GUS activity in the sepals of young buds was very high and decreased as the flowers matured (**Figure 1-2 H**). The activity in siliques also decreased in their middle part during elongation.

Mechanical wounding and MeJA treatment enhanced the expression of *AtHPL* (Matsui et al. 1999); therefore, it was assumed that expression of *AtHPL* was under the control of the JA-signaling pathway. COI1 is an F-box protein essential to transduce JA signaling through a specific binding of JA-Ile (Katsir et al. 2008; Mosblech et al. 2011; Wasternack & Hause 2013). DAD1 is a lipase essential to form JA in filaments and anthers (Ishiguro et al. 2001). When the GUS activity under the control of the *AtHPL* promoter was examined with a mutant lacking active COI1 or DAD1 (*coi1* or *dad1*, respectively), the GUS activity was much lower than that found in the flowers of Col-0 (**Figure 1-2 C, D, F, G, and I**). However, there was still weak but substantial GUS activity with *coi1* and *dad1* at the rim parts of carpels and sepals. Thus, deficiency of active COI1 or DAD1 seemed to suppress the intensity of GUS activity, but did not affect the spatial profile of the activity.
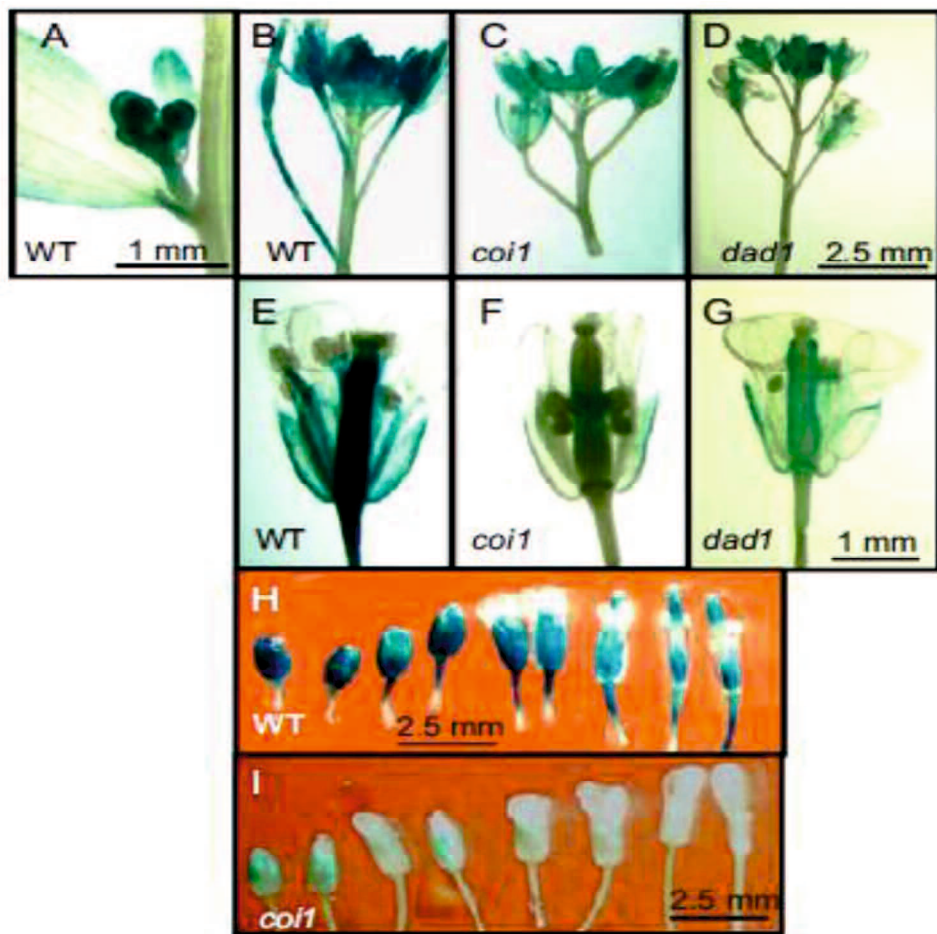
Figure 1-2. GUS activity in floral organs of transgenic *A. thaliana* plants. GUS activity derived from *pAtHPL::GUS* in floral organs of wild-type (Col-0) Arabidopsis (A, B, E, H), *coi1*(C, F, I), and *dad1* (D, G) was detected with GUS staining.

1.3.3   The ability to form GLV in flowers

To clarify whether HPL is active in flowers, we examined GLV formation in flowers before and after freeze–thaw treatment to facilitate extensive tissue disruption and compared GLV formation with that in leaves (**Figure 1-3**). The amounts of GLV formed and emitted from intact flowers were as low as 0.5 μmol g FW^{-1}, and they were several folds lower than those emitted from intact leaves. The GLV compositions were similar between flowers and leaves: (*Z*)-3-hexen-1-yl acetate and (*Z*)-3-hexen-1-ol were the major GLVs emitted out from both organs

14

when they were intact. When the flowers were disrupted through the freeze–thaw treatment, emission of GLVs, especially (*Z*)-3-hexenal, increased significantly. The composition of GLVs emitted from disrupted flowers was similar to that found in disrupted leaves (**Figure 1-3**; Matsui et al. 2012).
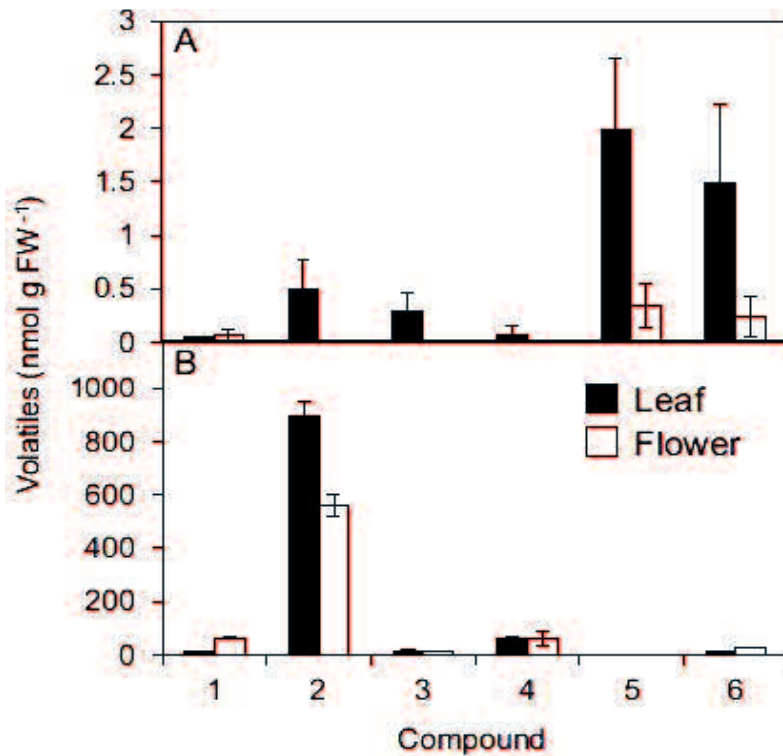
Figure 1-3. GLVs formed from intact and freeze-thaw–disrupted flowers and leaves. GLVs emitted from intact (A) and freeze-thaw–disrupted (B) flowers (white bars) and leaves (black bars) were collected with an SPME fiber, and quantified with gas chromatography–mass spectrometry. 1: *n*-hexanal, 2: (*Z*)-3-hexenal, 3: 1-penten-3-ol, 4: (*E*)-2-hexenal, 5: (*Z*)-3-hexen-1-yl acetate, 6: (*Z*)-3-hexen-1-ol. Values are given as means ± standard error.

1.3.4   Expression patterns of AtHPL gene after mechanical wounding

Classical studies showed that transcript levels of *AtHPL* and *AtAOS* increased after mechanical wounding (Bate et al. 1998; Kubigsteltig et al. 1999; Matsui et al. 1999). Here, we validated the previous results with higher spatial resolution using the GUS assay system. When

the *pHPL::GUS* transgenic Arabidopsis was grown for 8 days aseptically in a plate with agar nutrients, weak expression of GUS was found throughout the cotyledons, with a tendency for higher expression at the rim parts (**Figure 1-4**). At 30 min after mechanical wounding of one of the cotyledons, high GUS expression was observed at the rim parts. The high expression at the rim parts continued for approximately 24 h after mechanical wounding. The intensity and profile of GUS expression was similar in the other undamaged cotyledons. After 24 h, the GUS expression spread to the interior parts of both cotyledons. The emerging true leaves also showed intense GUS activity; however, the mid-vein of the leaves showed little activity.

The intact 8-day-old cotyledon of *pHPL::GUS/coi1* showed weaker GUS staining than that of *pHPL::GUS/Col-0*. Mechanical wounding increased the GUS activity at the rim part, but with an intensity that was much lower than that found with the reporter system with Col-0 background. The higher GUS activity persisted for least 24 h after wounding.

Expression of GUS under the control of the *AtAOS* promoter was also examined under the same conditions employed for *pHPL::GUS* to precisely compare the spatiotemporal expression profiles of these two genes. As reported previously (Kubigsteltig et al. 1999), GUS expression was barely detectable in intact Arabidopsis plants (**Figure 1-4**). Significant GUS expression was observed at 3 h after mechanical wounding. GUS expression was relatively constant in the lamina, with intense expression in the veins. There was no specific GUS induction around the wound site, even though intense GUS expression was observed around the wound site when the same reporter system was examined with tobacco (*Nicotiana tabacum*) plants (Kubigsteltig et al.1999). The expression profile was similar until 24 h after mechanical wounding. Slight GUS expression could be found at the base of the cotyledons, but expression in the other systemic cotyledons was not significant.
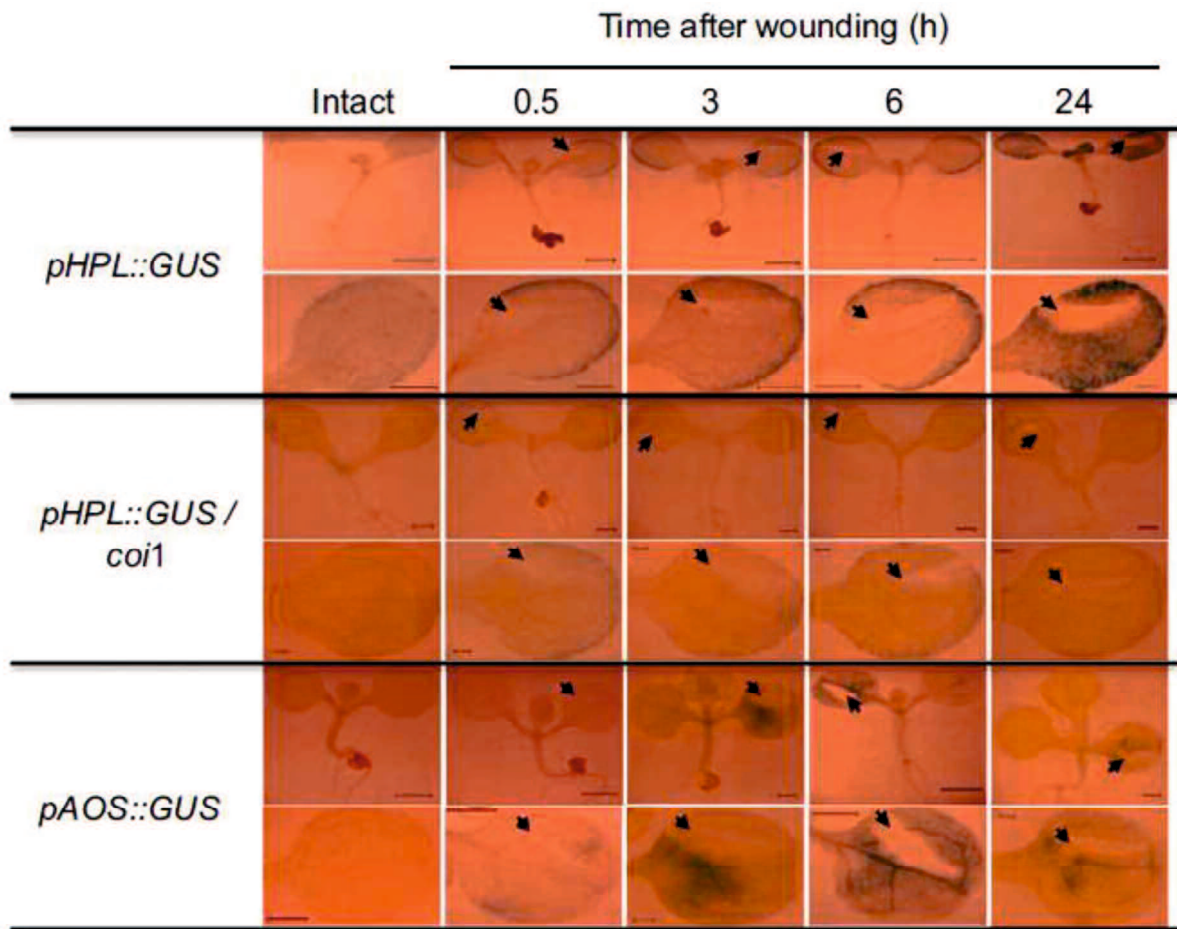
Figure 1-4. GUS activity in seedlings of transgenic *A. thaliana* plants after mechanical wounding. GUS activity derived from *pAtHPL::GUS* with wild-type (Col-0) and *coi1* and from *pAtAOS::GUS* with wild-type (C24) was detected with GUS staining after pressing one side of a cotyledon once with forceps. The wounded place is shown with arrows.

1.3.5   Oxylipin analysis in mid-vein and lamina of Arabidopsis leaves

The GUS reporter assay shown above indicated that *AtHPL* and *AtAOS* showed distinct spatiotemporal expression patterns after mechanical wounding. The most remarkable difference was observed in the vascular tissues, where GUS activity was almost absent with *pAtHPL::GUS*, while the most intense GUS activity was observed with *pAtAOS::GUS* after mechanical

17

wounding. To examine whether this spatial specificity correlates with spatial distribution of abilities to form GLVs and JAs, we mechanically wounded one side of 4-week-old Arabidopsis ecotype *No-0* leaves using a scalpel without touching the mid-veins and harvested the middle part containing the mid-veins and the other side of the leaves for determination of GLVs and JAs (**Figures 1-5 and 1-6**).

The amounts of GLVs from each part of leaves were determined by collecting volatiles emitted from the tissue sections after freeze–thaw disruption, using a SPME fiber for 30 min at 25 °C (**Figure 1-5**). Just after mechanical wounding (30 s), each leaf part showed substantial ability to form GLVs. With this procedure, *n*-hexanal, (*E*)-2-hexenal, (*Z*)-3-hexenal, and (*Z*)-3-hexen-1-ol were detected as major volatiles, and among them, (*Z*)-3-hexenal was the most abundant, as previously reported (Matsui et al. 2012). Among the sections, the lamina parts showed higher abilities to form GLVs than the mid-vein parts, except for (*Z*)-3-hexen-1-ol. Mechanical wounding resulted in little change in the GLV forming ability, even though the GUS activity observed with the reporter system significantly increased after mechanical wounding (**Figure 1-4**).

The amounts of oxylipins formed from the AOS pathway, namely, JA and JA-Ile, were also determined (**Figure 1-6**). JA and JA-Ile remained at a low level just after mechanical wounding, but their amounts increased transiently at 30 min after wounding. The transient accumulation of JA and JA-Ile peaking at 30 min after wounding was found only in the directly wounded lamina. Both JA and JA-Ile decreased thereafter, and at 24 h after wounding, they returned to the base level.
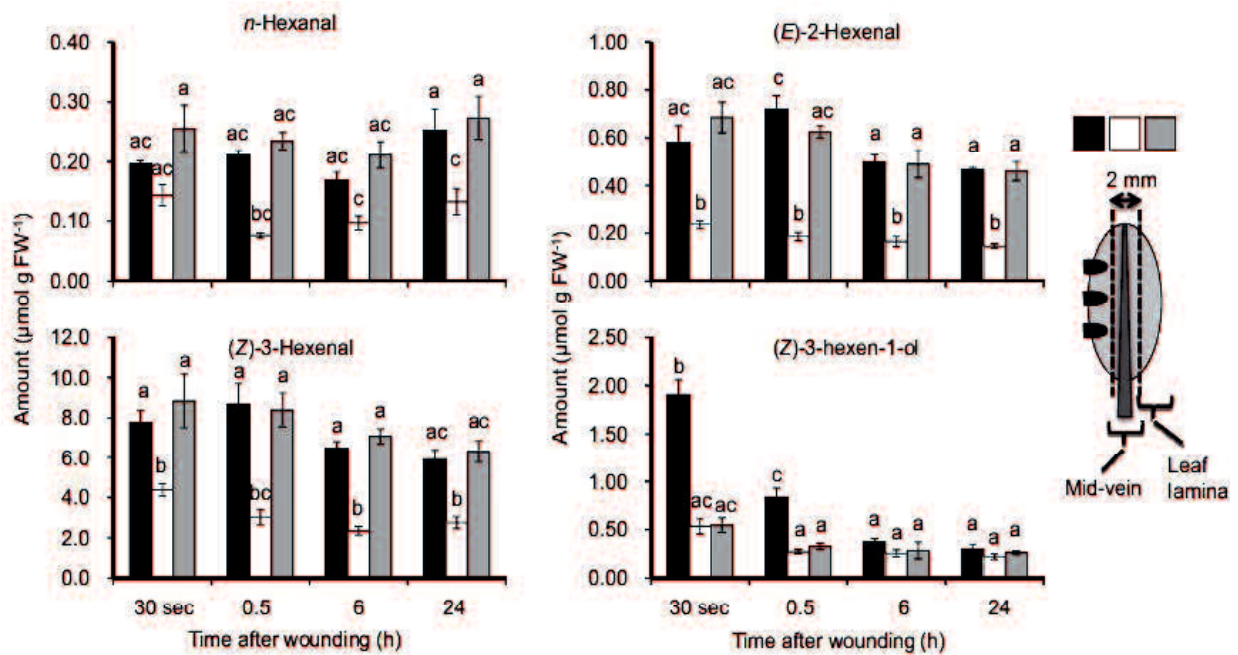
Figure 1-5. The ability to form GLVs in each section of the leaf after mechanical wounding. After applying a mechanical wound to leaf lamina of a 4-week-old Arabidopsis (No-0) plant with forceps, the leaf was dissected into directly injured lamina section (black bars), mid-vein section (white bars), and the other side of the lamina (grey bars) as shown with the diagram on the right. After freezing at −80 °C, the sections were thawed at 25 °C for 10 min. Thereafter, the volatiles formed were collected with an SPME fiber for 30 min at 25 °C. Values are given as means ± standard error (n = 3). The letters indicate significant differences between the mid-vein and leaf lamina (analysis of variance, Scheffé test, $P < 0.05$).
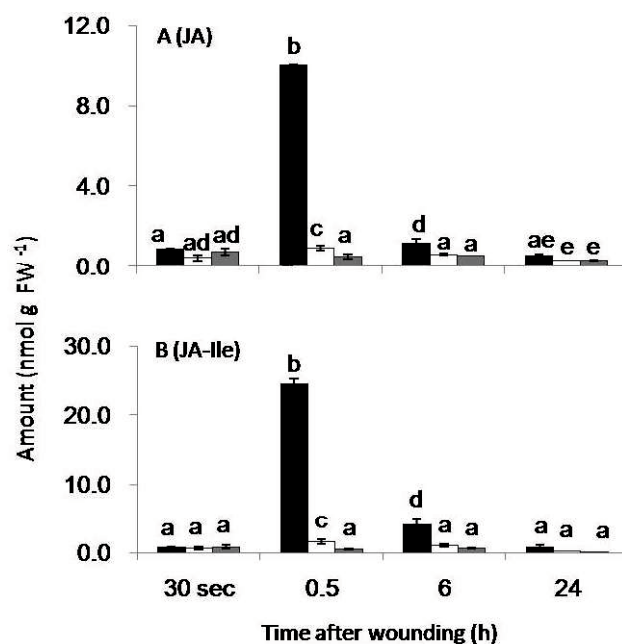
Figure 1-6. Amounts of JA and JA-Ile in each section of a leaf after mechanical wounding. Leaves of Arabidopsis (No-0) were wounded on one side of the leaf lamina. The leaf was then dissected into a directly injured lamina section (black bars), a mid-vein section (white bars), and the other side of the lamina (grey bars) as shown in Figure 5. The amounts of JA (A) and JA-Ile (B) were determined with LC-MS/MS. Values are given as means ± standard error (n = 3).

19

1.4 Discussion

Among the oxylipin branch pathways, the AOS and HPL are involved in the two major plant stress response pathways. These two branches might compete for the same substrate, 13-HPOT (Taurino et al. 2013), because HPL and AOS show similar substrate specificity; however, the physiological functions associated with their end products are distinct. Their endocellular localization might be one way to avoid the competition. The chloroplast protein database dedicated to sub-plastidial localization (PPDB [Plant protein database] and AT_Chloro) indicated that AtAOS is targeted to the envelope and thylakoids of chloroplasts. On the other hand, HPLs show diverse localization patterns; in some plants, HPLs are localized to the lipid bodies (Mita et al. 2005), the outer envelope of chloroplasts (Froehlich et al. 2001), and the stroma (Bonaventure 2014); in some cases, no specific localization in a particular organelle is observed (Phillips & Galliard 1978; Shibata et al. 1995b; Noordermeer et al. 2000). TargetP prediction for AtHPL indicated a cytoplasmic localization, while ChloroP prediction indicated a 34-amino acid chloroplast transit peptide. PPDB suggested a location on the outer envelope; however, this has not been confirmed experimentally. Probably the fact that HPL in Col-0, the most commonly used Arabidopsis ecotype for proteomic analysis, has a 10-nucleotide deletion in its first exon resulting in an inactive truncated protein (Duan et al. 2005) hindered identification of HPL through proteomic analysis. In this study, in vivo GFP fusion assays showed that the N-terminal 34 amino acid (derived from *No-0* ecotype) of AtHPL almost exclusively transported the fusion protein to the chloroplasts in the epidermal layer of Arabidopsis leaves. Even though it is still possible for the two CYP74 enzymes to be segregated at the level of sub-chloroplast membrane or even within the same membrane (Mita et al. 2005), the close localization of the two enzymes sharing the same substrate would cause disordered competition, especially when the

enzymes form their products in the disrupted tissues for the rapid oxylipin burst (Matsui 2006; Glauser et al. 2008, 2009). These results prompted us to compare the spatiotemporal expression patterns of these two genes.

Based on the results obtained with *pAtHPL::GUS* reporter system, we found that the promoter of *AtHPL* was active in floral organs, especially in peduncles, carpels, filaments, and sepals. Kubigsteltig et al. (1999) reported that the promoter activity of *AtAOS* was high at the pollen sacs and at the base of filaments. Apparently, the tissue specificity of AtHPL expression was largely distinct from that of AtAOS, except for the base of filaments; thus, the two enzymes could form their products from shared substrate (13-HPOT) mostly without competition. For example, pollen sacs must be important organs for JA formation, because JA is essential for pollen maturation and anther dehiscence (Ishiguro et al. 2001). There was little GUS activity in the pollen sacs of the *pAtHPL::GUS* plants, while the sacs were among most intensely stained organs in *pAtAOS::GUS* plants (Kubigsteltig et al. 1999). In the absence of HPL, AOS uses 13-HPOT exclusively, in a controlled manner, to adjust the best timing of pollen maturation.

As expected from the data obtained with transcript analyses, expression of GUS in *pAtHPL::GUS* was highly suppressed in an Arabidopsis mutant lacking the JA-signaling component (*coi1*) and the mutant lacking a lipase essential to JA formation in floral organs (*dad1*). DAD1 is specifically expressed in filaments and is involved in JA formation in floral organs, but is hardly involved in JA formation of Arabidopsis leaves, especially after wounding (Ellinger et al. 2010). Therefore, extensive suppression of GUS activity in *coi1* and *dad1* suggested that expression of *AtHPL* in peduncles, carpels and sepals was regulated by the JA (or JA-Ile) formed by DAD1 at the filaments, but not by JAs formed at the other organs. If this is the case, there should be a system to transport JA and/or JA-Ile from filaments to the other tissues of

the floral organs. It is also possible that a secondary signal molecule, formed depending on DAD1 and COI1 in filaments, might be a mobile signal directly inducing *AtHPL* expression in the other parts of the floral organs.

GLVs formed in intact flowers were low, and Arabidopsis self-pollinates; therefore, HPL in Arabidopsis may not be directly involved in recruiting pollinators. Instead, based on the fact that GLVs are extensively formed only after disruption of flowers, HPL in floral organs might have an important role in defense against herbivores and necrotrophic pathogens, as reported with caryophyllene synthase in Arabidopsis flowers (Huang et al. 2012).

Wound-inducible increases in *HPL* and *AOS* transcript levels have been documented in Arabidopsis (Bate et al. 1998; Laudert & Weiler 1998; Kubigsteltig et al. 1999; Matsui et al. 1999; Howe et al. 2000). Topological analysis using the GUS assay system showed that the spatiotemporal expression pattern of *AtHPL* after mechanical wounding was different from that of *AtAOS*. The present study showed that *AtHPL* is largely expressed in the mesophyll cells at the rim part of cotyledons, whereas *AtAOS* is preferentially expressed in the vasculature. The expression of *AtAOS* in the vascular tissues corresponded to the data reported by Kubigsteltig et al. (1999). Thus, it can be concluded that the spatiotemporal expression of *AtHPL* and *AtAOS* after mechanical wounding is regulated differently.

A transient increase in the amounts of JA and JA-Ile after mechanical wounding was found only in wounded leaf lamina. By contrast, high GUS activity was observed with *pAtHPL::GUS* plants at the other side of lamina and even at the other systemic cotyledon after mechanical wounding. This suggested that local accumulation of JA/JA-Ile was not a prerequisite for induction of *AtHPL* expression. Taken together with the fact that the GUS activity of *pAtHPL::GUS* was suppressed extensively in coi1 background, we hypothesized that

the expression of *AtHPL* is not directly regulated by JA/JA-Ile at the places where it was upregulated, but is regulated by an as-yet-unknown factor that is formed at the wounded site depending on COI1 after mechanical wounding.

GLVs, including (*E*)-2-hexenal, (*Z*)-3-hexenal, *n*-hexanal, as well as their corresponding alcohols or esters, are produced from mechanically wounded plant tissues (Hatanaka 1993; Matsui et al. 2012). After wounding, (*Z*)-3-hexenal as well as *n*-hexanal are the first products formed extensively in disrupted tissues, and they are converted into (*Z*)-3-hexen-1-ol and *n*-hexan-1-ol in the intact tissues adjacent to the wounds (Matsui et al. 2012). In the present study, the ability to form GLVs in the leaf lamina was shown to be higher than that in the mid-veins (**Figure 1-5**). We estimated the amounts of GLVs after freeze–thaw disruption; therefore, C6-aldehydes were the most abundant GLVs. C6-aldehydes have been reported to have insecticidal, fungicidal, and bactericidal activities (Hamilton-Kemp et al. 1992; Croft et al. 1993; Hammond et al. 2000; Vancanneyt et al. 2001; Nakamura & Hatanaka 2002; Hubert et al. 2008; Kishimoto et al. 2008), and thus they play a protective role in plant defense. The distinct spatial expression of HPL and accumulation of GLVs at the rim part of the leaf lamina may contribute to the ad hoc defense in plants upon tissue disruption, especially that caused by chewing insects. In our experiment, however, there was no increase in the abilities to form GLVs in the rim part of leaf lamina, even though GUS activity increased after mechanical wounding. The supply of substrate (13-HPOT) might be a limiting factor to determine the ability. By contrast, there are several reports indicating that formation and/or emission of some GLVs, such as (*Z*)-3-hexen-1-ol or (*Z*)-3-hexen-1-yl acetate, are enhanced after herbivore damage and mechanical wounding (D'Auria et al. 2007; Chehab et al. 2008). Thus, it was conceivable that induction of the HPL gene after mechanical wounding has an important role in forming a subset of GLVs, C6-alcohol, and C6-

acetate, which were largely involved in indirect defense or plant–plant interaction. To further test this hypothesis, quantification of each GLV emitted from each leaf section should be carried out. A technique to examine volatile emission from one leaf, or even from a small section of a leaf, should be developed in the future.

References

Arimura G, Matsui K, Takabayashi J. 2009. Chemical and molecular ecology of herbivore-induced plant volatiles. Proximate factors and their ultimate functions. Plant Cell Physiol. 50: 911-923.

Avdiushko S, Croft KPC, Brown GC, Jackson DM, Hamilton-Kemp TR, Hiderbrand D. 1995. Effect of volatile methyl jasmonate on the oxylipin pathway in tobacco, cucumber, and Arabidopsis. Plant Physiol. 109: 1227-1230.

Bate NJ, Sivasankar S, Moxon C, Riley JM, Thompson JE, Rothstein SJ. 1998. Molecular characterization of an Arabidopsis gene encoding hydroperoxide lyase, a cytochrome P-450 that is wound inducible. Plant Physiol. 117: 1393-1400.

Bonaventure G. 2014. Lipases and the biosynthesis of free oxylipins in plants. Plant Signaling Behav. 3: 9.

Brioudes F, Joly C, Szécsi J. 2009. Jasmonates control late development stages of petal growth in *Arabidopsis thaliana*. Plant J. 60: 1070-1080.

Chehab EW, Kaspi R, Savchenko T, Rowe H, Neger-Zakharov F, Kliebenstein D, Dehesh K. 2008. Distinct roles of jasmonates and aldehydes in plant-defense responses. PLoS One. 3: e1904.

Chehab EW, Raman G, Walley JW, Perea JV, Banu G, Theng S, Dehesh K. 2006. Rice HYDROPEROXIDE LYASES with unique expression patterns generate distinct aldehydes signatures in Arabidopsis. Plant Physiol. 141: 121-134.

Chiu W, Niwa Y, Zeng W, Hirano T, Kobayashi H, Sheen J. 1996. Engineered GFP as a vital reporter in plants. Curr Biol. 6: 325-330.

Creelman RA, Mullet JE. 1997. Biosynthesis and action of jasmonates in plants. Annu Rev Plant Physiol Mol Biol. 48: 355-381.

Croft KPC, Juttner F, Slusarenko AJ. 1993. Volatile products of the lipoxygenase pathway evolved from *Phaseolus vulgaris* (L.) leaves inoculated with *Pseudomonas syringae* pv *phaseolicola*. Plant Physiol. 101: 13-24.

D'Auria JC, Pichersky E, Schaub A, Hansel A, Gershenzon J. 2007. Characterization of BAHD acyltransferase responsible for producing the green leaf volatile (Z)-3-hexen-1-yl acetate in *Arabidopsis thaliana*. Plant J. 49: 194-207.

Duan H, Huang MY, Palacio K, Schuler MA. 2005. Variations in CYP74B2 (hydroperoxide lyase) gene expression differentially affect hexenal signaling in the Columbia and Landsberg *erecta* ecotypes of Arabidopsis. Plant Physiol. 139: 1529–1544.

Ellinger D, Stingl N, Kubigsteltig II, Bals T, Juenger M, Pollman S, Berger S, Schenemann D, Mueller MJ. 2010. Dongle and defective in anther dehiscence1 lipase are not essential for wound- and pathogen-induced jasmonate biosynthesis: redundant lipases contribute to jasmonate formation. Plant Physiol. 153: 114-127.

Erb M, Meldau S, Howe GA. 2012. Role of phytohormones in insect-specific plant reactions. Trends in Plant Sci. 17: 250-259.

Feussner I and Wasternack C. 2002. The lipoxygenase pathway. Annu Rev Plant Biol. 53: 275-297.

Froehlich JE, Itoh A, Howe GA. 2001. Tomato allene oxide synthase and fatty acid hydroperoxide lyase, two cytochrome P450s involved in oxylipin metabolism, are targeted to different membranes of chloroplast envelope. Plant Physiol. 125: 306-317.

Glauser G, Dubugnon L, Mousavi SA, Rudaz S, Wolfender J-L, Farmer EE. 2009. Velocity estimates for signal propagation leading to systemic jasmonic acid accumulation in wounded Arabidopsis. J Biol Chem. 284: 34506-34513.

Glauser G, Grata E, Dubugnon L, Rudaz S, Farmer EE, Wolfender J-L. 2008. Spatial and temporal dynamics of jasmonate synthesis and accumulation in Arabidopsis in response to wounding. J Biol Chem. 283: 16400-16407.

Grechkin AN, Hamberg M. 2004. The "heterolytic hydroperoxide lyase" is an isomerase producing a short-lived fatty acid hemiacetal. Biochim Biophys Acta. 1636: 47-58.

Hamilton-Kemp TR, McCracken CTJ, Loughrin JH, Andersen RA, Hildebrand DF. 1992. Effect of some natural volatile compounds on the pathogenic fungi *Alternaria alternata* and *Botrytis cinerea*. J Chem Ecol. 18: 1083-1091.

Hammond DG, Rangel S, Kubo I. 2000. Volatile aldehydes are promising broad-spectrum postharvest insecticides. J Agric Food Chem. 48: 4410-4417.

Hatanaka A. 1993. The biogeneration of green odor by green leaves. Phytochemistry. 34: 1201-1218.

Hause B, Wasternack C, Strack D. 2009. Jasmonates in stress responses and development. Phytochemistry. 70: 1483-1484.

Howe GA, Lee GI, Itoh A, Li L, DeRocher AE. 2000. Cytochrome P450-dependent metabolism of oxylipins in tomato:cloning and expression of allene oxide synthase and fatty acid hydroperoxide lyase. Plant Physiol. 123: 711-724.

Howe GA, Schilmiller AL. 2002. Oxylipin metabolism in response to stress. Curr Opin Plant Biol. 50: 230-236.

Huang M, Sanchez-Moreiras AM, Abel C, Sohrabi R, Lee S, Gershenzon J, Tholl D. 2012. The major volatile organic compound emitted from *Arabidopsis thaliana* flowers, the sesquiterpene (E)-β-caryophyllene, is a defense against a bacterial pathogen. New Phytol. 193: 997-1008.

Hubert J, Münzbergová Z, Santino A. 2008. Plant volatile aldehydes as natural insecticides against stored-product beetles. Pest Manag Sci. 64: 57-64.

Ishiguro S, Kawai-Oda A, Ueda J, Nishida I, Okada K. 2001. The defective in anther dehiscence1 gene encodes a novel phospholipase A1 catalyzing the initial step of jasmonic acid biosynthesis, which synchronized pollen maturation, anther dehiscence, and flower opening in Arabidopsis. Plant Cell. 13: 2191-2209.

Katsir L, Chung HS, Koo AJK, Howe GA. 2008. Jasmonate signaling: a conserved mechanism of hormone sensing. Curr Opin Plant Biol. 11: 428-435.

Kishimoto K, Matsui K, Ozawa R, Takabayashi J. 2008. Direct fungicidal activities of C6-aldehydes are important constituents for defense responses in Arabidopsis against *Botrytis cinerea*. Phytochemistry. 69: 2127-2132.

Knopf RR, Feder A, Mayer K, et al. 2012. Rhomboid proteins in the chloroplast envelope affect the level of allene oxide synthase in *Arabidopsis thaliana*. Plant J. 72: 559-571.

Kohlmann M, Bachmann A, Weichert H, Kolbe A, Balkenhohl T, Wasternack C, Feussner I. 1999. Formation of lipoxygenase-pathway-derived aldehydes in barley leaves upon methyl jasmonate treatment. Eur J Biochem. 260: 885-895.

Kubigsteltig I, Laudert D, Weiler E. 1999. Structure and regulation of *Arabidopsis thaliana* allene oxide synthase gene. Planta. 208: 463-471.

Matsui K, Sugimoto K, Mano J, Ozawa R, Takabayashi J. 2012. Differential metabolisms of green leaf volatiles in injured and intact parts of a wounded leaf meet distinct ecophysiological requirements. PLoS ONE. 7: e36433.

Matsui K, Toyota H, Kajiwara T, Kakuno T, Hatanaka A. 1991. A fatty acid hydroperoxide cleaving enzyme, hydroperoxide lyase, from tea leaves. Phytochemistry. 30: 2109-2113.

Matsui K, Wilkinson J, Hiatt B, Knauf V, Kajiwara T. 1999. Molecular cloning and expression of Arabidopsis fatty acid hydroperoxide lyase, from tea leaves. Phytochemistry 40: 477-481.

Matsui K. 2006. Green leaf volatiles. Hydroperoxide lyase pathway of oxylipin metabolism. Curr Opin Plant Biol. 9: 274-280.

Mita G, Quarta A, Fasano P, De Paolis A, Di sansebastiano GP, Perrotta C, Iannacone R, Belfield E, Hughes R, Tsesmetzis N, et al. 2005. Molecular cloning and characterization of an almond 9-hydroperoxide lyase, a new CYP74 targeted to lipid bodies. J Exp Bot. 56: 2321-2333.

Mosblech A, Feussner I, Heilmann I. 2009. Oxylipins. Structurally diverse metabolites from fatty acid oxidation. Plant Physiol Biochem. 47: 511-517.

Mosblech A, Thurow C, Gatz C, Feussner I, Heilmann I. 2011. Jasmonic acid perception by COI1 involves inositol polyphosphates in *Arabidopsis thaliana*. Plant J. 65: 949–957.

Nakamura S, Hatanaka A. 2002. Green-leaf-derived C6 aroma compounds with potent antibacterial action that act on both gram-negative and gram-positive bacteria. J Agric Food Chem. 50: 7639-7644.

Nelson DR. 1999. Cytochrome P450 and the individuality of species. Arch Biochem Biophys, 369: 1-10.

Noordermeer MA, Van Dijken AJ, Smeekens SC, Veldink GA, Vliegenthart JF. 2000. Characterization of three cloned and expressed 13-hydroperoxide lyase isoenzymes from alfalfa with unusual N-terminal sequences and different enzyme kinetics. Eur J Biochem. 267: 2473-2482.

Noordermeer MA, Veldink GA, Vliegenthart JF. 1999. Alfalfa contains substantial 9-hydroperoxide lyase activity and 3Z:2E-enal isomerase. FEBS Lett. 443: 201-204.

Nyambura MC, Matsui K, Kumamaru T. 2011. Establishment of an efficient screening system to isolate rice mutants deficient in green leaf volatile formation. J Plant Interact. 6: 185-186.

Phillips DR, Galliard T. 1978. Flavor biogenesis: partial purification and properties of a fatty acid hydroperoxide cleaving enzyme from fruits of cucumber. Phytochemistry. 17: 355-358.

Savchenko T, Kolla VA, Wang CQ, Nasafi Z, Hicks DR, Phadungchob B, Chehab WE, Brandizzi F, Froehlich J, Dehesh K. 2014. Functional convergence of oxylipin and abscisic acid pathways controls stomatal closure in response to drought. Plant Physiol. 164: 1151-1160.

Shibata Y, Matsui K, Kajiwara T, Hatanaka A. 1995a. Fatty acid hydroperoxide lyase is a heme protein. Biochem Biophys Res Commun. 207: 438-443.

Shibata Y, Matsui K, Kajiwara T, Hatanaka A. 1995b. Purification and properties of fatty acid hydroperoxide lyase from green bell pepper fruits. Plant Cell Physiol. 36: 147-156.

Sivasankar S, Sheldrick B, Rothstein SJ. 2000. Expression of allene oxide synthase determines defense gene activation in tomato. Plant Physiol. 122: 1335-1342.

Song WC, Brash AR. 1991. Purification of an allene oxide synthase and identification of the enzyme as a cytochrome P-450. Science. 252: 781-784.

Staswick PE, Lehman CC. 1999. Jasmonic acid-signaled responses in plants. In: Agrawal AA, Tazun S, Bent E, editor. Induced plant defenses against pathogens and herbivores. American Phytopathological Society. p. 117-136.

Sugimoto K, Matsui K, Iijima Y, Akakabe Y, Muramoto S, Ozawa R, Uefune M, Sasaki R, Alamgir KM, Akitake S. 2014. Intake and transformation to a glycoside of (Z)-3-hexenol from infested neighbors reveals a mode of plant odor reception and defense. Proc Natl Acad Sci USA. 111: 7144–7149.

Tanaka Y, Nishimura K, Kawamukai M, Oshima A, Nakagawa T. 2013. Redundant function of two Arabidopsis COPII components, AtSec24B and AtSec24C, is essential for male and female gametogenesis. Planta. 238: 561-575.

Taurino M, De Domenico D, Bonsegna S, Santino A. 2013. The hydroperoxide lyase branch of the oxylipin pathway and green leaf volatiles in plant/insect interaction. J Plant Biochem Physiol. 1: 102.

Vancanneyt G, Sanz C, Farmaki T, Paneque M, Ortego F, Castanera P, Sanchez-Serrano JJ. 2001. Hydroperoxide lyase depletion in transgenic potato plants leads to an increase in aphid performance. Proc Natl Acad Soc USA. 98: 8139-8144.

Wasternack C and Hause B. 2013. Jasmonates: biosynthesis, perception, signal transduction and action in plant stress response, growth and development. An update to the 2007 review in Annals of Botany. Ann Botany. 111: 1021-1058.

Weigel D, Glazerbrook J. 2002. Arabidopsis: a laboratory manual. Cold Spring Harbor (NY): Cold Spring Harbor Laboratory Press.

Xie DX, Feys BF, James S, Nieto-Rosto M, Turner JG. 1998. COI1: an Arabidopsis gene required for jasmonate regulated defense and fertility. Science. 280: 1091-1094.

Ziegler J, Keinanen M, Baldwin IT. 2001. Herbivore-induced allene oxide synthase transcripts and jasmonic acid in *Nicotiana attenuata*. Phytochemistry. 58: 729-738.

Appendix

Table 1-1: Parameters used to detect JA, D₂JA, OPDA and JA-Ile by LC-MS/MS. DP, declustering potential; EP, energy potential; CEP, collision energy potential; CE, collision energy; CXP, Collision Cell Exit Potential

Compound	Q1 mass (Da)	Q3 mass (Da)	DP (V)	EP (V)	CEP (V)	CE (V)	CXP (V)
JA	209.083	58.5	-60	-7	-12	-22	-58
D₂JA	211.111	58.8	-50	-8.5	-16	-22	-4
OPDA	290.905	165.2	-45	-10.5	-14	-28	-2
JA-Ile	321.935	130	-60	-8.5	-26	-34	-2
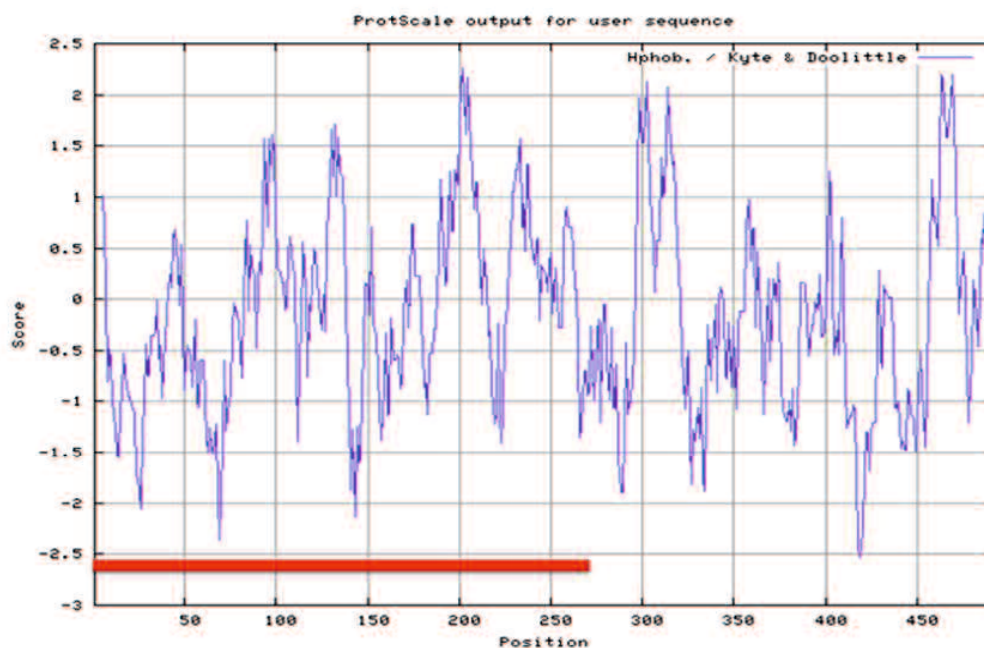
Figure 1-7. Hydropathy plot of AtHPL (Kyte and Doolittle). The region fused to GFP is shown in red line.
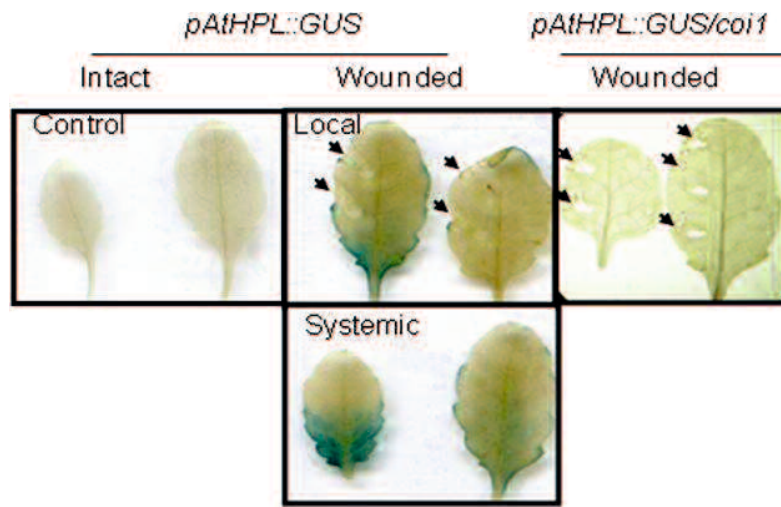
Figure 1-8. GUS activity in transgenic *A. thaliana* plants after mechanical wounding. GUS activity derived from *pAtHPL::GUS* with wild-type (Col-0) and *coi1* was detected with GUS staining after pressing one side of a leaf with forceps. The wounded place is shown with arrows.
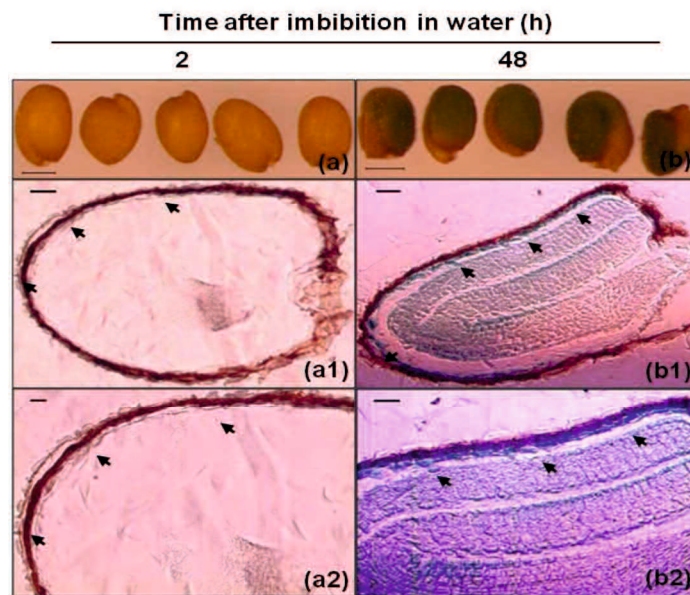
Figure 1-9. HPL promoter expression patterns in *pHPL::GUS* imbibed seeds. HPL promoter-driven GUS expression in (a) 2 h, (b) 48 h imbibed *pHPL::GUS* seeds (bar, 1 mm). Seeds were embedded in paraffin plast before slicing using a microtome. (a1) Longitudinal section (6 µm) and (a2) close-up of 2 h imbibed *pHPL::GUS* seed. (b1) Longitudinal section (6 µm) and close-up (b2) of 48 h imbibed *pHPL::GUS* seed. Black arrowheads show the aleurone layer. Scale bar, 10 µm.

2   CHAPTER TWO

(*E*)-2-hexenal promotes susceptibility to *Pseudomonas syringae* by activating jasmonic acid pathways in *Arabidopsis*

Abstract

Green leaf volatiles (GLVs) are C6-molecules – alcohols, aldehydes, and esters – produced by plants upon herbivory or during pathogen infection. Exposure to this blend of volatiles induces defense-related responses in neighboring undamaged plants, thus assigning a role to GLVs in regulating plant defenses. Here we compared *Arabidopsis thaliana* ecotype *Landsberg erecta* (*Ler*) with a *hydroperoxide lyase* line, *hpl1*, unable to synthesize GLVs, for susceptibility to *Pseudomonas syringae pv. tomato* (DC3000). We found that the growth of DC3000 was significantly reduced in the *hpl1* mutant. This phenomenon correlated with lower jasmonic acid (JA) levels and higher salicylic acid levels in the *hpl1* mutant. Furthermore, upon infection, the JA-responsive genes *VSP2* and *LEC* were only slightly or not induced, respectively, in *hpl1*. This suggests that the reduced growth of DC3000 in *hpl1* plants is due to the constraint of JA-dependent responses. Treatment of *hpl1* plants with (*E*)-2-hexenal, one of the more reactive GLVs, prior to infection with DC3000, resulted in increased growth of DC3000 in *hpl1*, thus complementing this mutant. Interestingly, the growth of DC3000 also increased in *Ler* plants treated with (*E*)-2-hexenal. This stronger growth was not dependent on the JA-signaling component MYC2, but on ORA59, an integrator of JA and ethylene signaling pathways, and on the production of coronatine by DC3000. GLVs may have multiple effects on plant–pathogen interactions, in this case reducing resistance to *Pseudomonas syringae* via JA and ORA59.

2.1 Introduction

Plants produce green leaf volatiles (GLVs), C6-aldehydes, C6-alcohols, and their acetates, through the lipoxygenase (LOX) and hydroperoxide lyase (HPL) pathways. Linoleic and linolenic acid are the substrates for dioxygenation and subsequent cleavage to obtain C6-volatile aldehydes that can be further modified by alcohol dehydrogenases (ADH), an isomerization factor and an acetyltransferase leading to the formation of a bouquet of these volatiles. Intact plants produce only trace amounts of GLVs, whereas these compounds are rapidly emitted in large amounts after wounding, herbivory or pathogen attack (Croft et al., 1993; Turlings et al., 1995; Fall et al., 1999; Shiojiri et al., 2000, 2006a; Heiden et al., 2003).

Green leaf volatiles have been reported to play important roles in different biological processes (Bate and Rothstein, 1998; Arimura et al., 2000; Farag and Paré, 2002; Engelberth et al., 2004; Farag et al., 2005; Ruther and Fürstenau, 2005; Ruther and Kleier, 2005). Herbivory induces very specific sets of GLVs that are perceived by natural predators of the herbivores (Kessler and Baldwin, 2001; Birkett et al., 2003; Gouinguené et al., 2005; Shiojiri et al., 2006a, b). Beside a role in indirect defenses, GLVs also act as airborne signalling molecules regulating plant defense responses. Several studies show that plants themselves upon exposure to GLVs respond by activating wound- and herbivore- induced defenses. Examples of this are found in *Zea mays* (maize), *Citrus jambhiri*, *Nicotiana attenuata* (tobacco), *Gossypium hirsutum*, *Lycopersicon esculentum* (tomato), and *Arabidopsis thaliana* plants where GLV perception induces the transcription of genes known to be involved in defense responses, or in biosynthesis of defense-related secondary metabolites (Bate and Rothstein, 1998; Arimura et al., 2001; Gomi et al., 2003; Weber et al., 2004; Farag et al., 2005; Kishimoto et al., 2005, 2006; Paschold et al., 2006), resulting in the production of defensive compounds (Zeringue, 1992; Bate and Rothstein,

1998; Farag and Paré, 2002; Engelberth et al., 2004; Farag et al., 2005; Ruther and Fürstenau, 2005; Kishimoto et al., 2006; Yan and Wang, 2006). Besides direct defense elicitation, exposure to GLVs, emitted from wounded leaves, has also been shown to prime systemic leaves for augmented defense responses upon future attacks (Engelberth et al., 2004; Kessler et al., 2006; Frost et al., 2007, 2008; Heil and Silva Bueno, 2007). Similarly, the (E)-2-hexenal released by rice upon planthopper infestation, induces expression of defense-related genes, increasing resistance to bacterial blight (Gomi et al., 2010). In some of these examples the effect of GLVs and jasmonic acid (JA) signalling have been linked (Engelberth et al., 2004; Halitschke et al., 2004; Kishimoto et al., 2006; Allmann et al., 2010; Tong et al., 2012).

Finally, GLVs possess fungicidal and bactericidal activity (Prost et al., 2005; Shiojiri et al., 2006b). Since GLVs are released after infection with pathogenic fungi and bacteria (Croft et al., 1993; Heiden et al., 2003; Shiojiri et al., 2006b), this suggests that a possible physiological role of these volatiles is to limit pathogen growth. Several observations support this hypothesis. For instance, upon infection with the pathogenic bacteria *Pseudomonas syringae*, *Phaseolus vulgaris* (lima bean) leaves release relatively high amounts of the C6-aldehyde, (E)-2-hexenal and the C6-alcohol (Z)-3-hexenol (Croft et al., 1993). Moreover, pre-treatment with the C6-aldehyde (E)-2-hexenal as well as genetic manipulation to enhance C6-volatile production, resulted in increased resistance against the necrotrophic fungus *Botrytis cinerea* in Arabidopsis, most likely as a result of both activation of defense responses and direct inhibition of fungal growth (Kishimoto et al., 2005; Shiojiri et al., 2006b).

Since all this evidence indicates a role for GLVs in regulating plant responses to bacterial pathogens and GLV levels have been shown to increase in plants upon infection with *Pseudomonas syringae* (Croft et al., 1993; Heiden et al., 2003), we decided to further dissect the

role of GLVs in the interaction of plants with this pathogen. Increased GLV levels could directly inhibit the pathogen and/or promote infection through downstream signalling favourable for the pathogen. *Pseudomonas syringae* pv. *tomato* DC3000 is a plant pathogen that enters leaves through stomata, multiplies in the apoplast, and produces necrotic lesions with chlorotic halos (Hirano and Upper, 2000). *Pseudomonas syringae* pv. *tomato* DC3000 (DC3000) causes bacterial speck on tomato (Cuppels, 1986), but also on *A. thaliana* (Whalen et al., 1991). DC3000 produces coronatine (COR), a toxin, responsible for chlorotic halos, which mimics the action of JA-isoleucine (JA-Ile), the active form of JA. With this phytotoxin DC3000 exploits the antagonistic interaction between JA and salicylic acid (SA) in order to shut down SA-dependent defenses that plant triggers to fight against *Pseudomonas* infections (Block et al., 2005; Glazebrook, 2005).

We especially focused on the role of (*E*)-2-hexenal during the Arabidopsis–Pseudomonas interaction. Although it is not the most abundant C6-volatile produced by HPL activity, (*E*)-2-hexenal is emitted during *Pseudomonas* ssp. infections in lima bean (Croft et al., 1993) and in tobacco (Heiden et al., 2003), and it has the highest bactericidal activity *in vitro* among oxylipins (Prost et al., 2005), likely because its α, β-unsaturated carbonyl moiety that can react with nucleophilic groups (Farmer and Davoine, 2007). Additionally, (*E*)-2-hexenal has been shown to induce several responses in Arabidopsis, including induction of defenses, inhibition of root growth and enhancement of resistance against the necrotrophic fungus *B. cinerea* (Bate and Rothstein, 1998; Kishimoto et al., 2005; Mirabella et al., 2008). In order to determine the role of GLVs in the responses against *Pseudomonas*, we set out to study Arabidopsis plants with and without a functional HPL (Shiojiri et al., 2012) and did complementation studies with (*E*)-2-hexenal. Remarkably we found that the presence of a working copy of HPL increased

susceptibility of Arabidopsis to DC3000. Treatment with (*E*)-2-hexenal also enhanced the susceptibility to this bacterial pathogen. We found evidence that this is mediated by the transcription factor ORA59, one of the main players in the JA-signalling pathways, and required the production of the bacterial toxin COR.

2.2   Materials and methods

2.2.1   *Plant lines*

Arabidopsis thaliana ecotype Columbia-0 (Col-0) and *Landsberg erecta* (*Ler*) were used. The *hpl1* mutant is an introgression line between Col-0 and *Ler* (Shiojiri et al., 2012). The mutant *myc2* (*jin1-7*; Verhage et al., 2011), the transgenic lines RNAi-ORA59 and the 35S::GUS plants (Pré et al., 2008) were all in the Col-0 background. Plants were grown in soil in a growth chamber at 21 °C, 70% relative humidity under an 11 h photo period with 100 μE s^{-1} m^{-2}.

2.2.2   *Bacterial population counts*

Bacteria were grown overnight at 28 °C in liquid King's broth (KB) medium (King et al., 1954) containing rifampicin (50 μg mL^{-1}) for the *Pseudomonas syringae* pv. *tomato* DC3000 strain, and kanamycin (100 μg mL^{-1}) for the cor^{-} DC3682 mutant strain, unable to produce COR (Ma et al., 1991). Plants were inoculated with either a low dose (OD600 of 0.0007), for bacterial growth assays, or a high dose (OD600 of 0.007), for qRT-PCR and hormone quantification, of the bacterial suspension, and bacteria (colony forming units, cfu) were counted as reported in Park et al. (2010).

2.2.3 Plant hormones extraction and quantification

For JA and SA quantification, 12 leaves were harvested, in pools of 4, from 12 different mock-infiltrated (10 mM $MgSO_4$) or bacteria-infiltrated plants in two independent experiments. To extract JA and SA, frozen leaf material (50–150 mg) was ground and homogenized in 0.5 mL 70% methanol, spiked with 200 ng of D_6JA and D_6SA (internal standards for extraction efficiency; CDN Isotopes, Canada[1]), with a Precellys24 automated lyser (Bertin Technologies[2]). Samples were homogenized twice by shaking at 6,000 rpm for 40 s and centrifuged at 10,000 g for 20 min at 4 °C. The supernatants of two extraction steps were pooled. Hormones were quantified by liquid chromatography–mass spectrometry (LC–MS) analysis on Varian 320 Triple Quad LC/MS/MS. Ten microliters of each sample were injected onto a C18 Pursuit 5 (50 mm × 2.0 mm) column (Varian) coupled to a double mass spectrometer in tandem (Varian 320 MS-MS[3]). The mobile phase comprised solvent A (0.05% formic acid) and solvent B (0.05% formic acid in methanol) as follows: 85% solvent A for 1 min 30 s (flow rate 0.4 mL min^{-1}), followed by 3 min in which solvent B increased till 98% (0.2 mL min^{-1}) which continued for 5 min 30 s with the same flow rate, followed by 2 min 30 s with increased flow rate (0.4 mL min^{-1}), subsequently returning to 85% solvent A in 1 min, conditions that were kept till the end of the run, in total 15 min. Compounds were detected in the electrospray ionization negative mode. Molecular ions [M-H]⁻ at m/z 137 and 209 and 141 and 213 generated from endogenous SA and JA and their internal standards, respectively, were fragmented under 12 V collision energy. The ratios of ion intensities of the irrespective daughter ions, m/z 93 and 97 and m/z 59 and 63, were used to quantify endogenous SA and JA, respectively.

2.2.4 *Quantitative RT-PCR*

For analysis of transcript levels, total RNA was isolated using Trizol from 10 infiltrated leaves, harvested from 10 different plants, in three independent experiments and treated with TurBo DNA free (Ambion[4]) to remove DNA. cDNA was synthesized from 1 µg of total RNA using M-MuLV reverse transcriptase (Fermentas[5]), as described by the manufacturer, in a 20 µL reaction that was diluted to 50 µL prior to using it for the real-time PCR. This was performed in a 20 µL volume containing 2 µL of cDNA, 0.4 pmol of specific primer sets for each gene and 10 µL of iTaq[TM] SYBR Green Super mix with ROX (Bio-Rad[6]). PCR conditions were as follows: 95 °C for 2 min 30 s (first cycle), 95 °C for 15 s and 60 °C for 30 s (40 cycles). To ensure amplification of a single product during the qRT-PCR reactions, a dissociation protocol was performed in which samples were slowly heated from 55 to 95 °C. qRT-PCR was performed using the ABI Prism 7000 real-time PCR detection system (Applied Biosystems) and the data were collected using software (ABI 7000 SDS version 1) provided by the supplier. Transcript levels were normalized to the levels of the *SAND* gene (At2g28390; Hong et al. 2010) and quantification was performed as described in previous work (Pfaffl, 2001). Primer sequences were as reported in (Anderson and Badruzsaufari, 2004; Czechowski et al., 2005; Park et al., 2010) for *PR1*, *VSP2*, LEC, and SAND, respectively.

2.2.5 *Trypan blue and Aniline blue staining*

Trypan blue staining solution was prepared by adding trypan blue to lactophenol (10 mL lactic acid, 10 mL glycerol, 10 mL phenol, and 10 mL distilled water) to a concentration of 2.5 mg mL^{-1}. Two volumes of ethanol were added to the trypan blue–lactophenol solution. To visualize plant cell death, mock and DC3000 infected leaf tissues were placed in plates

containing staining solution and heated in a microwave at intervals for 1 min. The plates were incubated for 2 h at room temperature, followed by destaining (three times) in chloral hydrate (2.5 g mL^{-1}). The leaf tissues were mounted in 70% glycerol for observations with a microscope. For detection of callose deposition, leaves were incubated for at least 24 h in 96% ethanol until all tissues were transparent and stained in 0.01% aniline blue in 0.15 M K_2HPO_4 (pH 8.5). Leaf tissues were incubated for 1.5 – 3 h, mounted on slides, and observed under an epifluorescence microscope (AF6000) with UV filter (excitation filter: BP 470/40 nm; emission filter: BP 525/50 nm).

2.2.6 Callose quantification

Callose was quantified from digital photographs as the number of white pixels, covering the whole leaf material, using Photoshop CS7 software. Contrast settings of photographs were adjusted to obtain an optimal separation of the callose signal from the back ground signal. Callose was selected automatically, using the "Color Range" tool. In cases in which the contrast settings resulted in significant loss of callose signal, due to high autofluorescence of vasculature tissue, callose was selected manually, using the "Magic Wand" tool of Photoshop CS7. Relative callose intensities were quantified as the number of fluorescent callose corresponding pixels relative to the total number of pixels covering plant material (Luna et al., 2011).

2.2.7 (E)-2-hexenal treatment

Plants were grown for 3 weeks under the conditions mentioned above before being exposed to volatiles. For the volatile treatment, 10 plants in single pots were placed into airtight glass desiccators (22 L). (E)-2-hexenal was diluted in methanol, and applied to a sterile cotton

swab, placed in an Erlenmeyer flask, between the plants in the desiccators to give a final concentration of 3 μM. For the control treatment, only methanol was applied. Plants were incubated in the desiccators for 24 h and subsequently taken out to be placed under the growth conditions described above for 1 h, prior to infiltration with bacteria or mock solution as mentioned above. (*E*)-2-hexenal was purchased from Sigma Aldrich, St. Luis, MO, USA.

2.3 Results

2.3.1 *hpl1 influences susceptibility to Pseudomonas syringae pv. tomato (DC3000)*

In order to determine whether the ability to synthesize GLVs had an effect on Arabidopsis susceptibility to pathogenic bacteria, we compared *Landsberg erecta* (*HPL*, *Ler*) and an introgression line between Col-0 and *Ler* that can synthesize only trace amounts of GLVs, *hpl1* (Shiojiri et al., 2012), for the susceptibility to *Pseudomonas syringae* pv. *tomato* DC3000. To ensure infection throughout the entire leaf, we used the syringe infiltration method since it overcomes stomatal defenses and maximizes the number of responding cells (de Torres Zabala et al., 2009), and bacterial populations were determined 72 hpi (hours post infection). **Figure 2-1** shows that DC3000 populations were lower in the *hpl1* line. The difference measured in bacterial population between *Ler* and *hpl1* (~ 4.6 fold) was statistically significant (*t*-test *P* < 0.05). This indicates that the *hpl1* line is less susceptible to DC3000 than *Ler*.

2.3.2 *hpl1 influences JA and SA levels during the infection with DC3000*

It is well known that balance between JA and SA is crucial for the interaction that will be established between a pathogen and its host (Spoel and Dong, 2008; Grant and Jones, 2009;

Pieterse et al., 2009). We therefore monitored the changes in JA and SA in *Ler* and the *hpl1* plants, prior to the bacterial population measurement, at 2, 24, and 48 hpi. As shown in **Figure 2-2A**, the levels of JA were up at 2 hpi in all treatments, most likely because of the mechanical damage caused by the inoculation with the syringe. At 24 hpi, this wound response was reset, as JA levels were very low, comparable to the mock inoculation. The situation changed at 48 hpi when JA levels increased in DC3000 infested leaves, in *Ler* approximately three fold higher than in *hpl1*. SA levels (**Figure 2-2B**) changed already at 24 hpi, with levels being approximately 1.7-fold higher in *hpl1* than in *Ler*, suggesting that SA-related defenses are activated earlier in *hpl1*. In *Ler*, the SA levels were higher than in *hpl1* at 48 hpi suggesting that these defenses are mounted later in *Ler*.
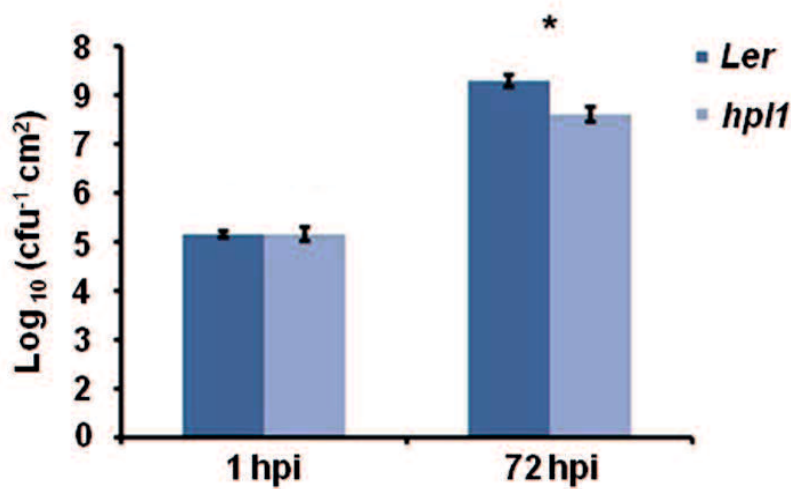
Figure 2-1. HPL influences bacterial growth. Bacterial populations of DC3000 in infected *Ler* and *hpl1* leaves 1 hour post infection (hpi) and 72 hpi. Values are the mean of 27 sets of two leaf disks from 20 plants. Error bars represent standard error. Bars annotated with an asterisk indicate significant differences among 72 hpi samples ($P < 0.05$, according to Student's *t*-test analysis). The data presented are from a representative experiment that was repeated four times with similar results.
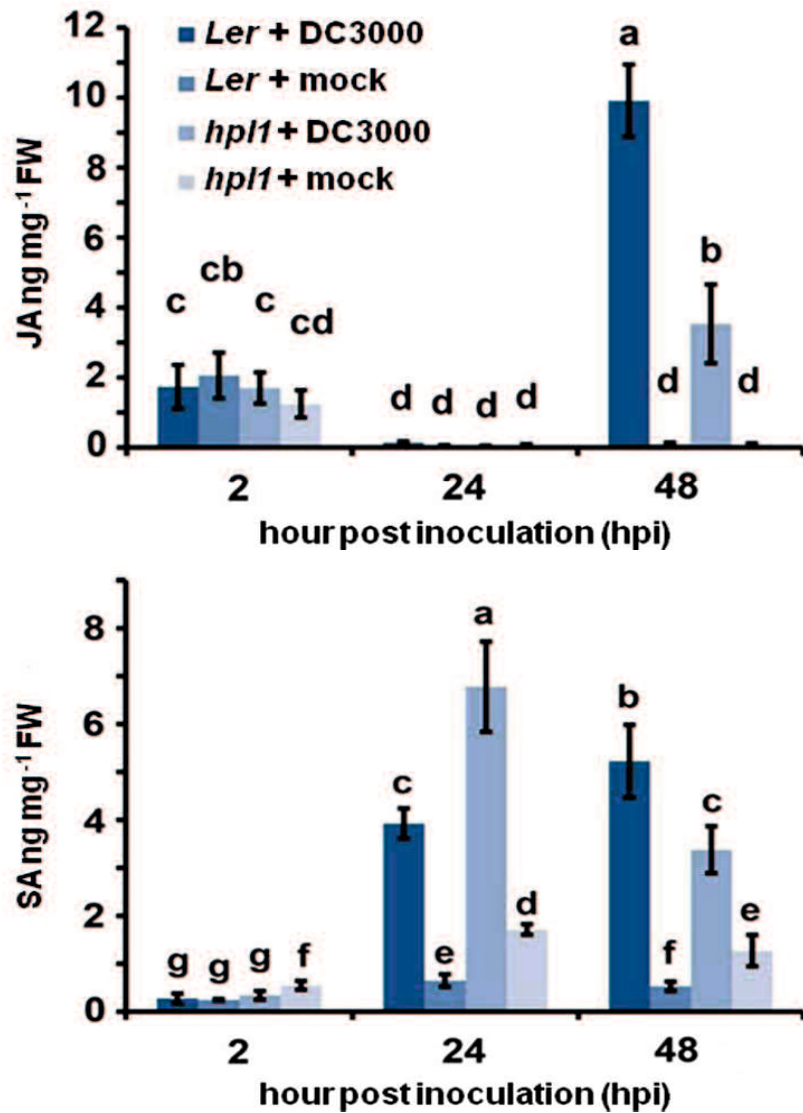
Figure 2-2. DC3000 infection results in higher JA levels in *Ler* plants and higher SA levels in *hpl1* plants. (A) JA levels in *Ler* and *hpl1* infected with DC3000 at 2, 24, and 48 hpi; (B) SA levels in *Ler* and *hpl1* plants infected with DC3000 at 2, 24, and 48 hpi. In both cases, the hormone levels in the 10 mM $MgSO_4$ (mock) infiltrated plants are also shown. For each time point and genotype, nine leaves were harvested, in pools of three from mock-infiltrated or bacteria-infiltrated plants and used for plant hormone quantification. Bars represent the mean of two independent experiments. Error bars represent standard error. Bars annotated with different letters indicate statistically different hormone levels [$P < 0.05$, according to analysis of variance (ANOVA), followed by a least significant difference (LSD) post hoc test].

2.3.3 *JA marker genes are less induced in hpl1 than Ler when infected with DC3000*

In order to determine whether the differences in hormone levels had an effect on the expression of relevant marker genes in our system, we performed qRT-PCR for genes downstream of JA and SA. We chose *VSP2* and *LEC* for JA (Potter et al., 1993; Penninckx et al., 1998; Thomma et al., 1998; Liu et al., 2005; Pré et al., 2008) and *PR-1* for SA (Bowling et al., 1997; Clarke et al., 2001). *PR1* expression was clearly induced by DC3000 at 48 hpi, however, to similar levels in *Ler* and *hpl1* plants (**Figure 2-8** in Appendix). In contrast, transcript levels of both *VSP2* and *LEC* at 48 hpi (and 24 hpi) were much lower in *hpl1* than in *Ler* (**Figures 2-3A, B**). This result is consistent with the observed lower JA levels in *hpl1* at 48 hpi (**Figure 2-2A**).
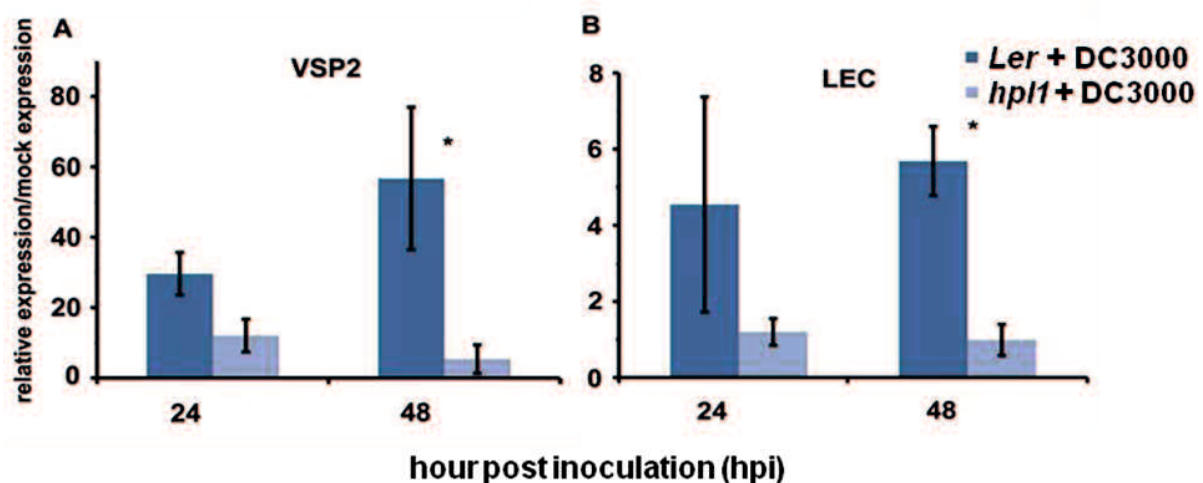
Figure 2-3. JA-dependent gene expression is higher in infected *Ler* plants. (A) VSP2 transcript levels and (B) LEC transcript levels were measured by qRT-PCR in *Ler* and *hpl1* infected with DC3000 at 24 and 48 hpi and normalized for SAND transcript levels. Bars represent the ratio between the transcript levels in infected and mock samples. Three infected or mock infiltrated leaves were harvested from three different plants and pooled for RNA isolation. Bars represent the mean of three independent experiments. Error bars represent standard error. Bars annotated with asterisk indicate significant differences among samples ($P < 0.05$, according to *t*-test analysis).

2.3.4 Ler and hpl1 differ in the number of dead cells and in callose deposition

To investigate further the differences between *Ler* and *hpl1* in mounting plant defense responses, we decided to look at the appearance of dead cells and callose deposition. Dead cells are indicative of programmed cell death (or the hypersensitive response, HR) and enhanced resistance, usually occurring when a pathogenic effector is recognized by the host (Alfano and Collmer, 1996), whereas callose is typically triggered by conserved pathogen associated molecular patterns (PAMPs), such as flagellin, at the sites of infection during the relatively early stages of pathogen invasion (Brown et al., 1998; Gómez-Gómez et al., 1999; Jones and Dangl, 2006). Dead cells appeared earlier and more frequently in the more resistant *hpl1* while callose deposition occurred earlier and more abundantly in the more susceptible *Ler* (**Figures 2-4A–C**). Dead cells appeared at day 2 in *hpl1*, whereas in *Ler* they were not present at all, even at day 3. *Ler* started to deposit callose massively at day 1, while much less papillae at this time could be observed in *hpl1*. Moreover, even at later stages of infection, at days 2 and 3, *Ler* showed more callose deposition than *hpl1*.

2.3.5 (E)-2-hexenal treatment increases susceptibility to DC3000

Since *hpl1* is unable to produce GLVs, we addressed the question whether application of GLVs would restore its susceptibility to DC3000 comparable to *Ler*. We chose to use the C6-aldehyde (*E*)-2-hexenal, one of the most active GLVs, and treated *hpl1* and *Ler* plants with 3 μM aerial (*E*)-2-hexenal or with the carrier methanol (MeOH) for the control treatment. **Figure 2-5A** shows that the treatment with the C6-aldehyde turned both *hpl1* and *Ler* more susceptible to DC3000, as bacterial populations increased about five-and nine fold, respectively, in the (*E*)-2-hexenal pre-treated leaves compared to the control pre-treatment (**Figure 2-5B**). Additionally, we

measured JA and SA levels in *Ler* and *hpl1* plants infected with DC3000 after pre-treatment with (*E*)-2-hexenal or MeOH. Although JA and SA levels increased 48 hpi after DC3000 infection, no significant differences in hormone levels were detected between the (*E*)-2-hexenal and the control treatment or between *Ler* and *hpl1* (**Figure 2-9** in Appendix).
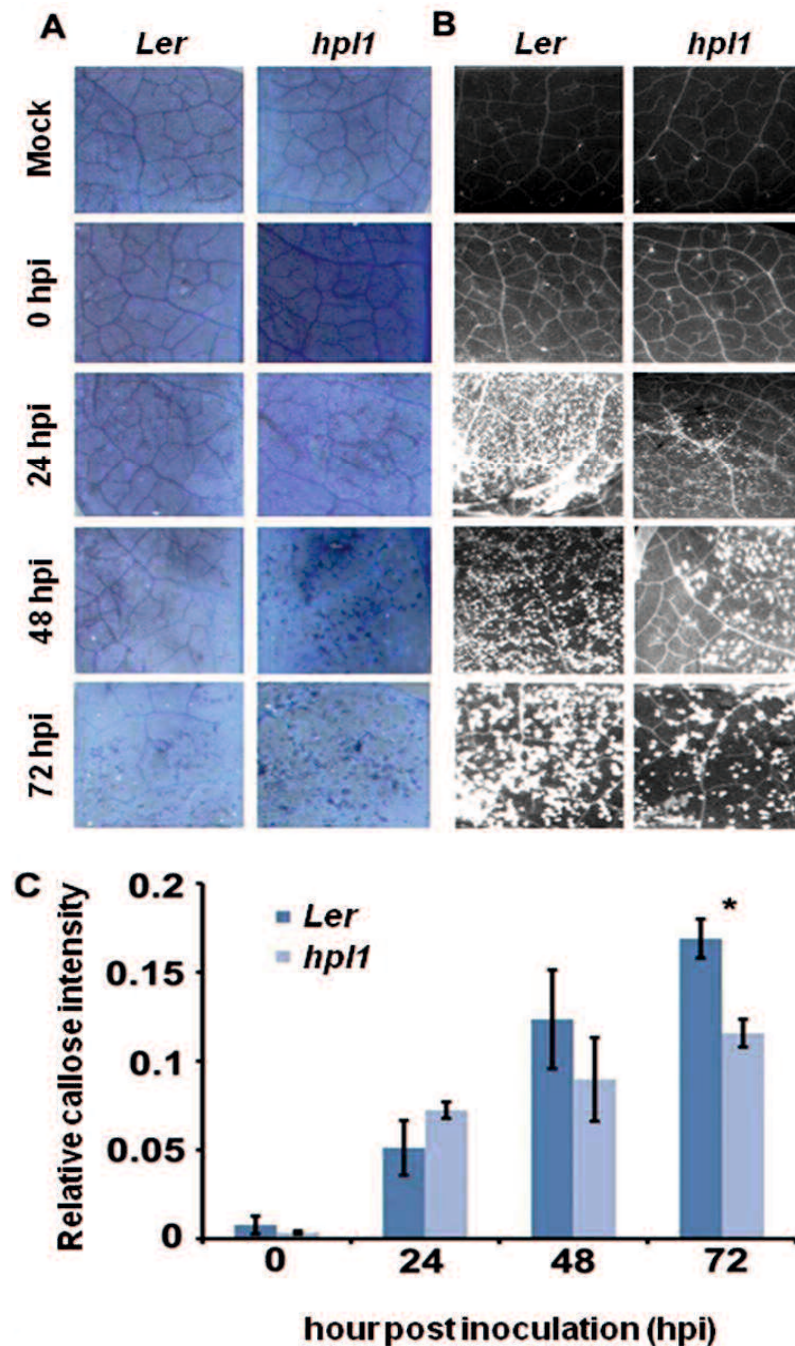
Figure 2-4. Dead cells and callose deposition are different in *Ler* and *hpl1*. (A) Trypan blue staining showing small clusters of dead cells in *hpl1* but not in *Ler* leaves infected with DC3000. (B) Aniline blue stained leaf tissues observed under UV illumination showing earlier and higher callose deposition in *Ler* than in *hpl1* leaves infected with DC3000. (C) Relative callose intensity. Bars represent the mean of three different experiments. Error bars represent standard error. Bars annotated with an asterisk indicate a significant difference among samples (*P* < 0.05, according to *t*-test analysis).
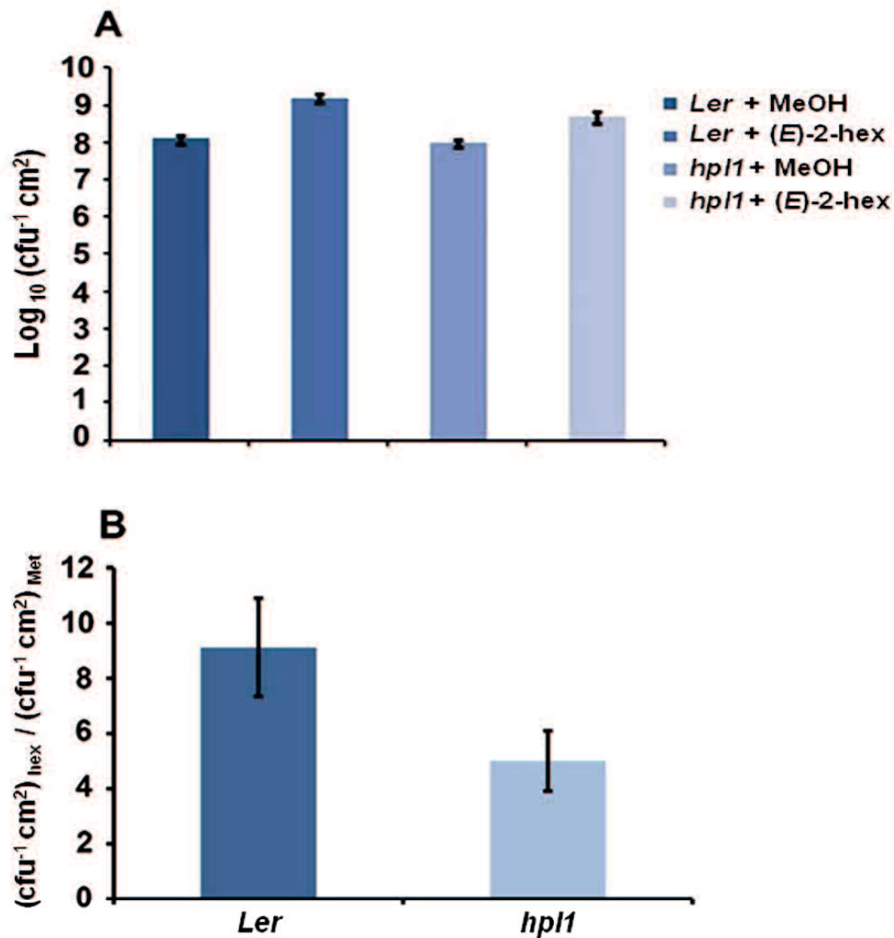
Figure 2-5. (*E*)-2-hexenal pre-treatment increases susceptibility to DC3000. (A) DC3000 populations in *Ler* and *hpl1* pre-treated with 3 μM (*E*)-2-hexenal or methanol was measured 72 hpi. Values are the mean of 16 sets of two leaf disks from 12 plants. Error bars represent standard error. The data presented are from a representative experiment that was repeated four times with similar results. All pre-treatments with (*E*)-2-hexenal were significantly different from the control treatment ($P < 0.05$, according to Student's *t*-test analysis). (B) Bars represent the ratio between cfu/cm^2 with (*E*)-2-hexenal pre-treatment and cfu/cm^2 with methanol pre-treatment (control). Values are the mean of three independent experiments. Error bars represent standard error.

2.3.6   The effect of (E)-2-hexenal on bacterial growth acts via ORA59

Since a functional HPL leads to higher susceptibility and higher JA levels upon DC3000 infection and (*E*)-2-hexenal pre-treatment increased susceptibility of Arabidopsis to DC3000 we

sought to elucidate part of the signalling pathways involved, by testing if Arabidopsis mutants in the JA-signalling pathway were still more susceptible to DC3000 after treatment with (*E*)-2-hexenal. We chose to analyze MYC2 and ORA59 impaired lines since these are the main players in regulating JA-dependent responses and are located in two different branches of the JA-signalling pathway (Lorenzo et al., 2003, 2004; Anderson and Badruzsaufari, 2004; Dombrecht et al., 2007; Oñate-Sánchezetal., 2007; Kazan and Manners, 2008; Pré et al., 2008). As shown in **Figure 2-6A**, *myc2* (*jin1-7*) plants were more resistant to DC3000 as has been reported (Fernández- Calvo et al., 2011). Moreover, *myc2* as well as wild-type plants showed increased susceptibility to DC3000 when pre-treated with (*E*)-2-hexenal, seemingly excluding a role for MYC2 in mediating this phenomenon. In contrast, the same assay performed on RNAi-ORA59 plants (Pré et al., 2008) showed that the bacterial populations increased significantly less in the ORA59 silenced plants compared to the corresponding control line after (*E*)-2-hexenal treatment (**Figure 2-6B**). This indicates an involvement of ORA59 in this response to (*E*)-2-hexenal.

2.3.7   The (E)-2-hexenal effect is coronatine dependent

Pseudomonas syringae pv. *tomato* strain DC3000 synthesizes COR (Mitchell, 1982), a phytotoxin that mimics JA-Ile (Thines et al., 2007; Yan et al., 2009), in order to antagonize the SA-dependent defenses (Brooks et al., 2005; Glazebrook, 2005). Therefore, we also determined whether the production of COR was necessary for DC3000 to proliferate more in (*E*)-2-hexenal treated plants. For this, *Ler* and *hpl1* plants were infected with the *Pseudomonas syringae* mutant strain DC3682 (Ma et al., 1991) that is unable to produce COR, after pre-treatment with (*E*)-2-hexenal or methanol. **Figure 2-7** shows that the bacterial populations of the *cor* mutant were only slightly, but significantly, higher in *Ler* or *hpl1* plants treated with (*E*)-2-hexenal compared

to the control plants, but that this increase was much lower than for DC3000 (**Figure 2-1**). Thus

COR seems to be necessary for DC3000 to benefit from the (*E*)-2-hexenal treatment.
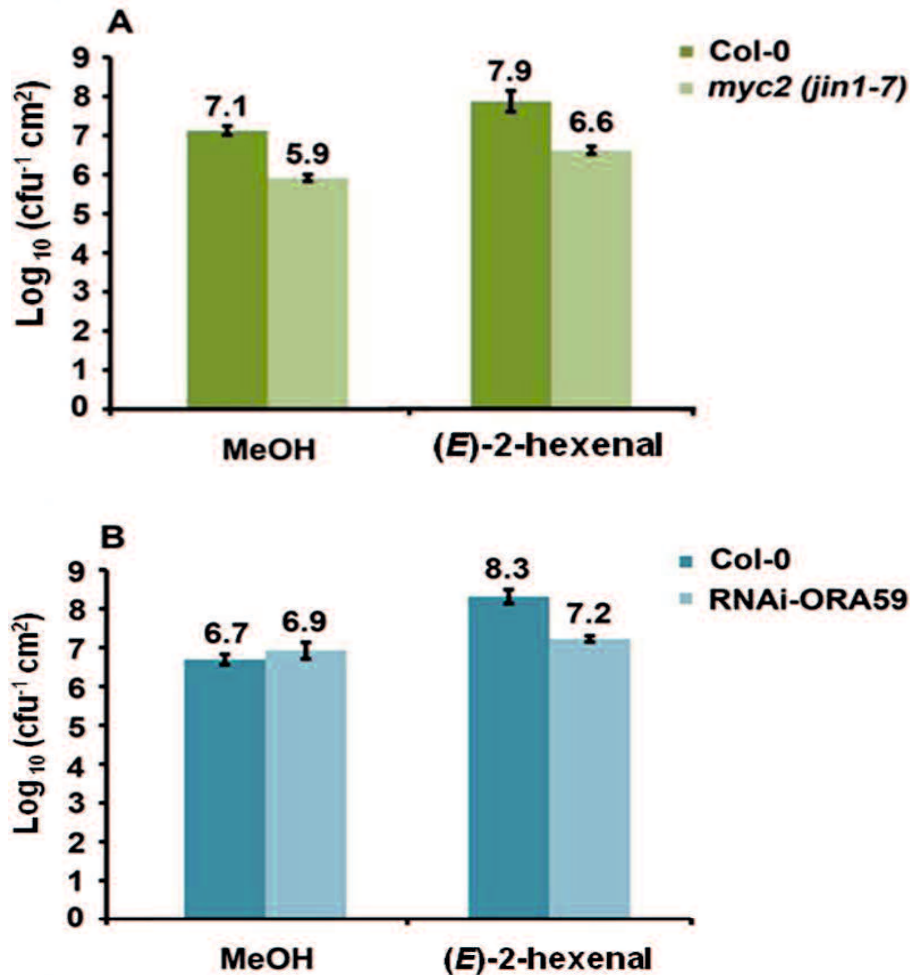
Figure 2-6. Reduction of *ORA59* expression influences (*E*)-2-hexenal effect on bacterial growth. (A) Bacterial populations of DC3000 in inoculated *myc2 (jin1-7)* and Col-0 leaves 72 hpi. Plants were pre-treated 24 h with 3 μM (*E*)-2-hexenal or methanol. (B) Bacterial populations of DC3000 in inoculated RNAi-ORA59 and 35S::GUS plants at 72 hpi. Plants were pre-treated with 3 μM (*E*)-2-hexenal or methanol for 24 h. Values are the mean of 24 sets of two leaf disks from 20 plants. Error bars represent standard error. All pre-treatments with (*E*)-2-hexenal were significantly different from the control treatment ($P < 0.05$, according to Student's *t*-test analysis), except for RNAi-ORA59. The data presented are from a representative experiment that was repeated three times with similar results.
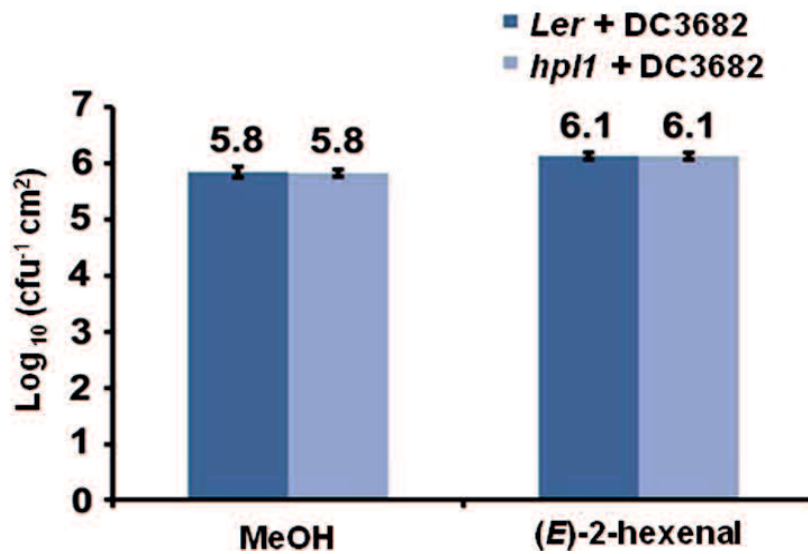
Figure 2-7. The effect of (*E*)-2-hexenal is partially dependent on coronatine. Bacterial populations of the *cor* mutant (DC3682) in inoculated *Ler* and *hpl1* leaves at 72 hpi. Plants were pre-treated 24 h with 3 μM (*E*)-2-hexenal or methanol. Values are the mean of 24 sets of two leaf disks from 20 plants. Error bars represent standard error. All pre-treatments with (*E*)-2-hexenal were significantly different from the control treatment ($P < 0.05$, according to Student's *t*-test analysis). The data presented are from a representative experiment that was repeated three times with similar results.

2.4 Discussion

Green leaf volatiles have received considerable attention for their ability to induce direct and indirect defense responses in plants and can be considered important players in the already complex network regulated during biotic stress. However the mechanisms, by which GLVs influence pathogenesis, and the signalling pathways involved in these responses, are not well known. To address this, we used *Ler* and its Arabidopsis introgression line, *hpl1*, lacking GLV synthesis, and analyzed their response during infection with the bacterial pathogen *Pseudomonas syringae* pv. *tomato* (DC3000). DC3000 was chosen because in some plant species such as lima bean and tobacco, infection triggers (*E*)-2-hexenal emission (Croft et al., 1993; Heiden et al.,

53

2003). We hypothesized that *hpl1* plants would be more susceptible to DC3000 since there is evidence that GLVs and (*E*)-2-hexenal have antimicrobial properties (Prost et al., 2005), induced defense-related genes or biosynthesis of defense-related secondary metabolites (Bate and Rothstein, 1998; Arimura et al., 2001; Gomi et al., 2003; Weber et al., 2004; Farag et al., 2005; Kishimoto et al., 2005, 2006; Paschold et al., 2006), and increase resistance against *B. cinerea* (Kishimoto et al., 2005). However, we found the opposite result: plants impaired in GLV production were more resistant to DC3000 (**Figure 2-1**). A similar result was very recently shown in rice where the mutant Os*hpl3*, not able to synthesize GLVs, was more resistant to *Xanthomonas oryzae* pv. *oryzae* (Tong et al., 2012). Subsequently, we investigated some of the mechanisms underlying this result by analyzing the levels of SA and JA since it is well known that these phytohormones and their antagonism are crucial for the development of pathogenesis in *Arabidopsis* (Spoel and Dong, 2008; Grant and Jones, 2009; Pieterse et al., 2009). Hormone measurements clearly showed that JA levels were much lower in *hpl1* than in *Ler* (**Figure 2-2A**). Conversely, *hpl1* showed an earlier induction of SA than *Ler* (**Figure 2-2B**). These data suggest that a non-functional *HPL* gene influences the JA-branch of the oxylipin pathway, leading to lower production of JA when Arabidopsi*s* is challenged with *Pseudomonas*. Thus, this is not related to substrate competition as previously shown in Arabidopsis where ectopic expression of *HPL* led to lower JA levels upon wounding (Chehab et al., 2006). Reduction of *HPL* expression in rice and *N. attenuata* also influenced JA levels but differently: Os*hpl3* and *asHPL1* had increased JA levels (Halitschke et al., 2004; Tong et al., 2012), in *N. attenuata* probably due to crosstalk between the GLV and JA pathway (Allmann et al., 2010).

Since JA-signalling downstream of COI1 occurs via two different branches, regulated by MYC2 or ORA59, we used markers for both branches to study their activation after DC3000

infection. *LEC*, a lectin-like gene, was used for the ORA59 pathway since it is induced by methyl-jasmonate and upon ORA59 overexpression (Schenk et al., 2000; Pré et al., 2008), while *VSP2* was used for the MYC2 pathway (Abe et al., 2003; Dombrecht et al., 2007). Both *VSP2* and *LEC* transcript levels were much lower in *hpl1* than in *Ler* (**Figures 2-3A, B**) concurrent with the lower JA levels. Thus DC3000 activates in *Ler*, with an active HPL unlike Col-0 (Duan et al., 2005), with which most DC3000 experiments are carried out, both branches of the JA-signalling pathway and antagonistic control of these distinct branches of the JA pathway (Verhage et al., 2011) is apparently minor. Transcript levels of the SA-marker *PR-1* were higher upon DC3000 infection, similarly in *hpl1* and *Ler* (**Figure 2-8** in Appendix), probably because the differences in SA levels between the two genotypes were not big enough to cause a difference. Thus it seems that the lower JA levels in *hpl1* plants leads to less activation of the JA-signalling pathways and renders them less susceptible to DC3000.

A hallmark of basal plant defenses to pathogen infection is the deposition of callose. PAMP-induced callose deposition has recently been defined with essential roles for the DC3000 type III effector HopM1 and COR suppressing callose deposition, the latter being, interestingly, partly COI1-independent (Geng et al., 2012). Our results showed that in *hpl1*, although with smaller bacterial populations than in *Ler*, clearly less callose was deposited (**Figures 2-4B, C**). Ethylene (ET) signalling it is crucial for callose deposition in response to flagellin (Clay et al., 2009). It is possible that this ET signalling is less activated in *hpl1*, leading to less callose deposition. Support for this comes from our complementation studies with the *hpl1* mutant, a response that is largely dependent on ORA59, a TF that integrates JA and ET signalling (**Figure 2-6B**). Perhaps related to this is the fact that DC3000 is apparently less effective in preventing cell death in *hpl1* than in *Ler* (**Figure 2-4A**), with fewer living cells producing less callose.

DC3000 apparently triggers in *hpl1* a higher rate of cell death, which is related to higher resistance (Jones and Dangl, 2006).

With the aim to overcome the *hpl1* phenotype in response to DC3000 infection, we decided to treat these, and *Ler*, plants with (*E*)-2-hexenal. The pre-treatment with 3 μM (*E*)-2-hexenal for 24 h prior to DC3000 infection made *hpl1* plants considerably more susceptible to DC3000 (**Figures 2-5A, B**). The increase in bacterial populations was about nine fold in *Ler* and five fold in *hpl1* plants. Thus *Ler* plants remained more susceptible to DC3000 than *hpl1* plants, most likely due to the functional HPL. Due to its high reactivity for being a reactive electrophile species (RES), (*E*)-2-hexenal, either induced during the HR or exogenously applied, can undergo conjugation to glutathione (GSH), leading to the formation of (*E*)-2-hexenal-GSH adducts in the form of 1-hexanol-3-GSH (Davoine et al., 2006; Mirabella et al., 2008). Conjugation to GSH is a well-known mechanism to inactivate reactive molecules (Coleman et al., 1997). Additionally, conjugation to cellular proteins has been reported to occur for several RES, including (*E*)-2-hexenal (Davoine et al., 2006; Myung et al., 2007; Dueckershoff et al., 2008; Mueller et al., 2008; Yamauchi et al., 2008). Therefore, we cannot exclude the possibility that, through conjugation, (*E*)-2-hexenal affects the function of proteins involved in the plant defense responses to DC3000, making Arabidopsis more susceptible to this pathogen. A similar effect has been reported for syringolin, a toxin with an unsaturated α, β carbonyl moiety, that makes it a RES, produced by, e.g., *Pseudomonas syringae* pv. *syringae*. This toxin specifically inhibits the proteasome in order to suppress host defenses (Groll et al., 2008; Schellenberg et al., 2010).

Analyses of phytohormone levels after treatment of (*E*)-2-hexenal and DC3000 infection showed that there were no statistically significant differences in SA and JA levels between control and treatment (**Figure 2-9** in Appendix). So far only in monocots (maize) an increase in

JA has been measured after a GLV treatment (Engelberth et al., 2004; Engelberth, 2011). In the JA-signalling pathway COI1 plays a central role and mutants in this gene are blocked in almost all JA responses (Feng et al., 2003; Devoto et al., 2005; Wang et al., 2008). Downstream of COI1, different TFs regulate specific JA-dependent responses: MYC2 and ORA59 are the main players involved. The MYC2 dependent branch is associated with wound response, responses against herbivores and is also regulated by abscisic acid (ABA; Lorenzo et al., 2003). This basic helix-loop-helix (bHLH) transcription factor regulates a large number of JA-responsive genes (Dombrecht et al., 2007), among which VEGETATIVE STORAGE PROTEIN 2 (VSP2; Liu et al., 2005). In the other branch, ORA59 integrates JA and ET signalling (Pré et al., 2008). Interestingly, in spite of the absence of difference in JA and SA levels, the higher susceptibility of Arabidopsis plants to DC3000 after (*E*)-2-hexenal treatment was dependent on ORA59. The DC3000 bacterial populations increased only slightly in ir-ORA59 plants after (*E*)-2-hexenal treatment as compared to control (35S::GUS) plants (**Figure 2-6B**), indicating the relevance of JA signalling, and perhaps ET signalling. A role for MYC2 in this process was excluded based on the fact that *myc2* mutants still responded to exogenous (*E*)-2-hexenal treatment (**Figure 2-6A**).

From the bacterial side we investigated whether the production of COR was necessary to benefit from the (*E*)-2-hexenal treatment. For this we employed *cor*, a COR-deficient strain, to infect plants, after the (*E*)-2-hexenal or control treatment. The result showed that there was a small but significant increase in bacterial populations of the *cor* strain after the (*E*)-2-hexenal treatment (**Figure 2-7**). Nevertheless this difference was much smaller than for DC3000, suggesting that COR is necessary for DC3000 to fully benefit from GLVs.

Our data show that a functional *HPL* in Arabidopsis promotes susceptibility to DC3000. This effect is partially mediated by ORA59 in the plant and by COR in the bacteria.

The question remains how DC3000 precisely exploits HPL or its products, GLVs or the C12 compounds that are also formed in the HPL pathway (Kallenbach et al., 2011), for its benefit. Since it is clear that some herbivores can lower *HPL* transcript levels (Halitschke et al., 2004; Savchenko et al., 2012), we propose that HPL maybe a target for DC3000 to employ in Arabidopsis, albeit to its own advantage.

References

Abe H, Urao T, Ito T, Seki M. 2003. Arabidopsis AtMYC2 (bHLH) and AtMYB2 (MYB) function as transcriptional activators in abscisic acid signaling. Plant Cell. 15: 63-78.

Alfano JR and Collmer A. 1996. Bacterial pathogens in plants: life up against the wall. Plant Cell. 3: 1683-1698.

Allmann S, Halitschke R, Schuurink RC, Baldwin IT. 2010. Oxylipin channelling in *Nicotiana attenuata*: lipoxygenase 2 supplies substrates for green leaf volatile production. Plant Cell Environ. 33: 2028-2040.

Anderson J and Badruzsaufari E. 2004. Antagonistic interaction between abscisic acid and jasmonate-ethylene signaling pathways modulates defense gene expression and disease resistance in. Plant Cell. 16: 3460-3479.

Arimura G, Ozawa R, Horiuchi J, Nishioka T, Takabayashi J. 2000. Herbivory-induced volatiles elicit defence genes in lima bean leaves. Nature. 406: 512-515.

Arimura G, Ozawa R, Shimoda T, Nishioka T, Boland W, Takabayashi J. 2001. Pant-plant interactions mediated by volatiles emitted from plants infested by spider mites. Biochem Syst Ecol. 29: 1049-1061.

Bate NJ, Rothstein SJ. 1998. C6-volatiles derived from the lipoxygenase pathway induce a subset of defense-related genes. Plant J. 16: 561-569.

Birkett MA, Chamberlain K, Guerrieri E, Pickett JA, Wadhams LJ, Yasuda T. 2003. Volatiles from whitefly-infested plants elicit a host locating response in the parasitoid, *Encarsia formosa*. J Chem Ecol. 29: 1589-1600.

Block A, Schmelz E, Jones JB, Klee HJ. 2005. Coronatine and salicylic acid: the battle between Arabidopsis and *Pseudomonas* for phytohormone control. Mol Plant Pathol. 6: 79-83.

Bowling SA, Clarke JD, Liu Y, Klessig DF, Dong X. 1997. The cpr5 mutant of Arabidopsis expresses both NPR1-dependent and NPR1-independent resistance. Plant Cell. 9: 1573-1584.

Brooks DMD, Bender CLC, Kunkel BNB. 2005. The *Pseudomonas syringae* phytotoxin coronatine promotes virulence by overcoming salicylic acid-dependent defences in *Arabidopsis thaliana*. Mol Plant Pathol. 6: 629-639.

Brown I, Trethowan J, Kerry M. 1998. Localization of components of the oxidative cross-linking of glycoproteins and of callose synthesis in papillae formed during the interaction between non-pathogenic strains of *Xanthomonas campestris* and French bean mesophyll cells. Plant J. 15: 333-343.

Chehab EW, Raman G, Walley JW, Perea JV, Banu G, Theng S, Dehesh K. 2006. Rice HYDROPEROXIDE LYASES with unique expression patterns generate distinct aldehydes signatures in Arabidopsis. Plant Physiol. 141: 121-134.

Clarke JD, Aarts N, Feys BJ, Dong X, Parker JE. 2001. Constitutive disease resistance requires EDS1 in the Arabidopsis mutants cpr1 and cpr6 and is partially EDS1-dependent in cpr5. Plant J. 26: 409-420.

Clay N, Adio A, Denoux C. 2009. Glucosinolate metabolites required for an Arabidopsis innate immune response. Science. 323: 95-101.

Coleman JOD, Randall R, Blake-Kalff MMA. 1997. Detoxification of xenobiotics in plant cells by glutathione conjugation and vacuolar compartmentalization: a fluorescent assay using monochlorobimane. Plant Cell Environ. 20: 449-460.

Croft K, Juttner F, Slusarenko A. 1993. Volatile products of the lipoxygenase pathway evolved from *Phaseolus vulgaris* (L.) leaves inoculated with *Pseudomonas syringae* pv. *phaseolicola*. Plant Physiol. 101: 13-24.

Cuppels DA. 1986. Generation and characterization of Tn5 insertion mutations in. Appl Environ Microbiol 51: 323–327.

Czechowski T, Stitt M, Altmann T. 2005. Genome-wide identification and testing of superior reference genes for transcript normalization in Arabidopsis. Plant Physiol. 139: 5-17.

Davoine C, Falletti O, Douki T, Iacazio G, Ennar N, Montillet JL, Triantaphylidés C. 2006. Adducts of oxylipin electrophiles to glutathione reflect a 13 specificity of the down stream lipoxygenase pathway in the tobacco hypersensitive response. Plant Physiol. 140: 1484-1493.

de Torres Zabala M, Bennett MH, Truman WH, Grant MR. 2009. Antagonism between salicylic and abscisic acid reflects early host-pathogen conflict and moulds plant defense responses. Plant J. 59: 375-386.

Devoto A, Ellis C, Magusin A, Chang HS, Chilcott C, Zhu T, et al. 2005. Expression profiling reveals COI1 to be a key regulator of genes involved in wound- and methyljasmonate-induced secondary metabolism, defense, and hormone interactions. Plant Mol Biol. 58: 497-513.

Dombrecht B, Xue GP, Sprague SJ, Kirkegaard JA, Ross JJ, Reid JB, et al. 2007. MYC2 differentially modulates diverse jasmonate-dependent functions in Arabidopsis. Plant Cell. 19: 2225-2245.

Duan H, Huang M, Palacio K, Schuler M. 2005. Variations in CYP74B2 (hydroperoxide lyase) gene expression differentially affect hexenal signalling in the Columbia and *Landsberg erecta* ecotypes of Arabidopsis. Plant Physiol. 139: 1529-1544.

Dueckershoff K, Mueller S, Mueller MJ, Reinders J. 2008. Impact of cyclopentanone-oxylipins on the proteome of *Arabidopsis thaliana*. Biochim Biophys Acta. 1784: 1975-1985.

Engelberth J. 2011. Selective inhibition of jasmonic acid accumulation by a small alpha-unsaturated carbonyl and phenidone reveals different modes of octadecanoid signalling activation in response to insect elicitors and green leaf volatiles in *Zea mays*. BMC Res Notes. 4:377. doi:10.1186/1756-0500-4-377.

Engelberth J, Alborn HT, Schmelz EA, Tumlinson JH. 2004. Airborne signals prime plants against insect herbivore attack. Proc Natl Acad Sci USA. 101: 1781-1785.

Fall R, Karl T, Hansel A, Jordan A, Lindiger W. 1999. Volatile organic compounds emitted after leaf wounding: on-line analysis by proton-transfer-reaction mass spectrometry. J Geophys Res Atmos. 104: 15963-15974.

Farag MA, Fokar M, Abd H, Zhang H, Allen RD, Paré PW. 2005. (Z)-3-hexenol induces defense genes and downstream metabolites in maize. Planta. 220: 900-909.

Farag MA, Paré PW. 2002. C6-green leaf volatiles trigger local and systemic VOC emissions in tomato. Phytochemistry. 61: 545-554.

Farmer EE, Davoine C. 2007. Reactive electrophile species. Curr Opin Plant Biol. 10: 380–386.

Feng S, Ma L, Wang X. 2003. The COP9 signalosome interacts physically with SCF[COI1] and modulates jasmonate responses. Plant Cell. 15: 1083-1094

Fernández-Calvo P, Chini A, Fernández-Barbero G, Chico JM, Gimenez-Ibanez S, Geerinck J, et al. 2011. The Arabidopsis bHLH transcription factors MYC3 and MYC4 are targets of JAZ repressors and act additively with MYC2 in the activation of jasmonate responses. Plant Cell. 23: 701-715.

Frost CJ, Appel HM, Carlson JE, De Moraes CM, Mescher MC, Schultz JC. 2007. Within-plant signalling via volatiles overcomes vascular constraints on systemic signalliing and primes responses against herbivores. Ecol Lett. 10: 490-498.

Frost CJ, Mescher MC, Carlson JE, De Moraes, CM. 2008. Plant defense priming against herbivores: getting ready for a different battle. Plant Physiol. 146: 818-824.

Geng X, Cheng J, Gangadharan A, Mackey D. 2012. The coronatine toxin of *Pseudomonas syringae* is a multifunctional suppressor of Arabidopsis defense. Plant Cell. 24: 4763-4774.

Glazebrook J. 2005. Contrasting mechanisms of defense against biotrophic and necrotrophic pathogens. Annu Rev Phytopathol. 43: 205–227.

Gómez-Gómez L, Felix G, Boller T. 1999. A single locus determines sensitivity to bacterial flagellin in *Arabidopsis thaliana*. Plant J. 18: 277-284.

Gomi K, Satoh M, Ozawa R, Shinonaga Y, Sanada S, Sasaki K, et al. 2010. Role of hydroperoxide lyase in white-backed planthopper (*Sogatella furcifera* Horváth)- induced resistance to bacterial blight in rice, *Oryza sativa* L. Plant J. 61: 46-57.

Gomi K, Yamasaki Y, Yamamoto H, Akimitsu K. 2003. Characterization of hydroperoxide lyase gene and effect of C6-volatiles on expression of genes of the oxylipin metabolism in *Citrus*. J Plant Physiol. 160: 1219-1231.

Gouinguené S, Pickett JA, Wadhams LJ, Birkett MA, and Turlings TCJ. 2005. Antennal electrophysiological responses of three parasitic wasps to caterpillar- induced volatiles from maize (*Zea mays mays*), cotton (*Gossypium herbaceum*), and cowpea (*Vigna unguiculata*). J Chem Ecol. 31: 1023-1038.

Grant MR and Jones JDG. 2009. Hormone (dis)harmony moulds plant health and disease. Science. 324: 750–752.

Groll M, Schellenberg B, Bachmann AS, Archer CR, Huber R, Powell TK, et al. 2008. A plant pathogen virulence factor inhibits the eukaryotic proteosome by a novel mechanism. Nature. 452: 755-758.

Halitschke R, Ziegler J, Keinänen M, Baldwin IT. 2004. Silencing of hydroperoxide lyase and allene oxide synthase reveals substrate and defense signalling crosstallk in *Nicotiana attenuata*. Plant J. 45: 35-46.

Heiden AC, Kobel K, Langebartels C, Schuh-Thomas G, Wildt J. 2003. Emission of oxygenated volatile organic compounds from plants part I: emission from lipoxygenase activity. J Atmos Chem. 45: 143-172.

Heil M, Silva Bueno JC. 2007. Within-plant signalling by volatiles leads to induction and priming of an indirect plant defense in nature. Proc Natl Acad Sci USA. 104: 5467–5472.

Hirano SS, Upper CD. 2000. Bacteria in the leaf ecosystem with emphasis on *Pseudomonas syringae* – a pathogen, ice nucleus, and epiphyte. Microbiol Mol Biol Rev. 64: 624–653.

Hong SM, Bahn SC, Lyu A, Jung HS, Ahn JH. 2010. Identification and testing of superior reference genes for a starting pool of transcript normalization in Arabidopsis. Plant Cell Physiol. 51: 1694-1706.

Jones JDG, Dangl JL. 2006. The plant immune system. Nature. 444: 323-329.

Kallenbach M, Gilardoni PA, Allmann S, Baldwin IT, Bonaventure G. 2011. C12 derivatives of the hydroperoxide lyase pathway are producd by product recycling through lipoxygenase-2 in *Nicotiana attenuata* leaves. New Phytol. 191: 1054-1068.

Kazan K, Manners JM. 2008. Jasmonate signaling: toward an integrated view. Plant Physiol. 146: 1459-1468.

Kessler A, Baldwin IT. 2001. Defensive function of herbivore-induced plant volatile emissions in nature. Science. 291: 2141-2144.

Kessler A, Halitschke R, Diezel C, Baldwin IT. 2006. Priming of plant defense responses in nature by airborne signaling between *Artemisia tridentata* and *Nicotiana attenuata*. Oecologia. 148: 280-292.

King EO, Ward MK, Raney DE. 1954. Two simple media for the demonstration of phycocyanin and fluorescein. J Lab Clin Med. 44: 301-307.

Kishimoto K, Matsui K, Ozawa R, Takabayashi J. 2005. Volatile C6-aldehydes and Allo-ocimene activate defense genes and induce resistance against *Botrytis cinerea* in *Arabidopsis thaliana*. Plant Cell Physiol. 46: 1093-1102.

Kishimoto K, Matsui K, Ozawa R, Takabayashi J. 2006. ETR1-, JAR1- and PAD2- dependent signalling pathways are involved in C6-aldehyde-induced defense responses. Plant Sci. 171: 415-423.

Liu Y, Ahn J, Datta S, Salzman R. 2005. Arabidopsis vegetative storage protein is an anti-insect acid phosphatase. Plant Physiol. 139: 1545-1556.

Lorenzo O, Chico J, Sánchez-Serrano JJ, Solano R. 2004. JASMONATE INSENSITIVE1 encodes MYC2 transcription factor essential to discriminate between different jasmonate-regulated defense responses in Arabidopsis. Plant Cell. 16: 1938-1950.

Lorenzo O, Piqueras R, Sánchez- Serrano JJ, Solano R. 2003. ETHYLENE RESPONSE FACTOR1 integrates signals from ethylene and jasmonate pathways in plant defense. Plant Cell. 15: 165-178.

Luna E, Pastor V, Robert J, Flors V, Mauch-Mani B,Ton J. 2011. Callose deposition: a mutlifaceted plant defense response. Mol Plant Microbe Interact. 24: 183-193.

Ma SW, Morris VL, Cuppels DA. 1991. Characterization of DNA region required for production of the phytotoxin coronatine by *Pseudomonas syringae* pv. *tomato*. Mol Plant Microbe Interact. 4: 69-74.

Mirabella R, Rauwerda H, Struys EA, Jakobs C, Triantaphylidès C, Haring MA, et al. 2008. The Arabidopsis her1 mutant implicates GABA in E-2-hexenal responsiveness. Plant J. 53: 197-213.

Mitchell R. 1982. Coronatine production by some phytopathogenic pseudomonads. Physiol Plant Pathol. 20: 83-89.

Mueller S, Hilbert B, Dueckershoff K, Roitsch T, Krischke M, Mueller MJ, et al. 2008. General detoxification and stress responses are mediated by oxidized lipids through TGA transcription factors in Arabidopsis. Plant Cell. 20: 768-785.

Myung K, Hamilton-Kemp TR, Archbold DD. 2007. Interaction with and effects on the profile of proteins of *Botrytis cinerea* by C6 aldehydes. J Agric Food Chem. 55: 2182-2188.

Oñate-Sánchez L, Anderson JP, Young J, Singh KB. 2007. AtERF14, a member of the ERF family of transcription factors, plays a nonredundant role in plant defense. Plant Physiol. 143: 400-409.

Park DH, Mirabella R, Bronstein PA, Preston GM, Haring MA, Lim CK, et al. 2010. Mutations in gamma-aminobutyric acid (GABA) transaminase genes in plants or *Pseudomonas syringae* reduce bacterial virulence. Plant J. 64: 318-330.

Paschold A, Halitschke R, Baldwin IT. 2006. Using 'mute' plants to translate volatile signals. Plant J. 45: 275-291.

Penninckx IA, Thomma BP, Buchala A, Métraux JP, Broekaert WF. 1998. Concomittant activation of jasmonate and ethylene response pathways is required for induction of a plant defensin gene in Arabidopsis. Plant Cell. 10: 2103-2113.

Pfaffl MW. 2001. A new mathematical model for relative quantification in real-time RT- PCR. Nucleic Acids Res. e45.

Pieterse CMJ, Leon-Reyes A, Van der Ent S, Van Wees SCM. 2009. Networking by small molecule hormones in plant immunity. Nat Chem Biol. 5: 308-316.

Potter S, Uknes S, Lawton K. 1993. Regulation of a hevein-like gene in Arabidopsis. Mol Plant Microbe Interact. 6: 680-685.

Pré M, Atallah M, Champion A, De Vos M, Pieterse CMJ, Memelink J. 2008. The AP2/ERF domain transcription factor ORA59 integrates jasmonic acid and ethylene signals in plant defense. Plant Physiol. 147: 1347-1357.

Prost I, Dhondt S, Rothe G. 2005. Evaluation of the antimicrobial activities of plant oxylipins supports their involvement in defense against pathogens. Plant Physiol. 139: 1902-1913.

Ruther J, Fürstenau B. 2005. Emission of herbivore-induced volatiles in absence of a herbivore-response of *Zea mays* to green leaf volatiles and terpenoids. Naturforsch C. 60: 743-756.

Ruther J and Kleier S. 2005. Plant-plant signaling: ethylene synergizes volatile emission in *Zea mays* induced exposure to (Z)-3-hexen-1-ol. J Chem Ecol. 31: 2217-2222.

Savchenko T, Pearse I, Ignatia L. 2012. Insect herbivores selectively suppress the HPL branch of the oxylipin pathway in host plants. Plant J. 73: 653-662.

Schellenberg B, Ramel C, Dudler R. 2010. *Pseudomonas syringae* virulence factor syringolin A counteracts stomatal immunity by proteasome inhibition. Mol Plant Microbe Interact. 23: 1287-1293.

Schenk PM, Kazan K, Wilson I, Anderson JP, Richmond T, Somerville SC, et al. 2000. Coordinated plant defense responses in Arabidopsis revealed by microarray analysis. Proc Natl Acad Sci USA. 97: 11655-11660.

Shiojiri K, Kishimoto K, Ozawa R, Kugimiya S, Urashimo S, Arimura G, et al. 2006a. Changing green leaf volatile biosynthesis in plants: an approach for improving plant resistance against both herbivores and pathogens. Proc Natl Acad Sci USA. 103: 16672-16676.

Shiojiri K, Ozawa R, Matsui K, Kishimoto K, Kugimiya S, Takabayashi J. 2006b. Role of the lipoxygenase/lyase pathway of host-food plants in the host searching behaviour of two parasitoid species, *Cotesia glomerata* and *Cotesia plutellae*. J Chem Ecol. 32: 969-979.

Shiojiri K, Ozawa R, Matsui K, Sabelis MW, Takabayashi J. 2012. Intermittent exposure of green leaf volatiles triggers a plant response. Sci Rep, 2: 378.

Shiojiri K, Takabayashi J, Yano S, Takafuji A. 2000. Flight response of parasitoids toward plant-herbivore complexes: a comparative study of two parasitoid -herbivore systems on cabbage plants. Appl Entomol Zool. 35: 87-92.

Spoel SH, Dong X. 2008. Making sense of hormone crosstalk during plant immune responses. Cell Host Microbe. 3: 348-351.

Thines B, Katsir L, Melotto M, Niu Y, Mandaokar A, Liu G, et al. 2007. JAZ repressor proteins are targets of the SCF(COI1) complex during jasmonate signalling. Nature. 448, 661-665.

Thomma BP, Eggermont K, Penninckx IA, Mauch-Mani B, Vogelsang R, Cammue BP, et al. 1998. Separate jasmonate-dependent and salicylate-dependent defense-response pathways in Arabidopsis are essential for resistance to distinct microbial pathogens. Proc Natl Acad Sci USA. 95: 15107-15111.

Tong X, Qi J, Zhu X, Mao B, Zeng L, Wang B, et al. 2012. The rice hydroperoxide lyase OsHPL3 functions in defense responses by modulating the oxylipin pathway. Plant J. 71: 763-775.

Turlings T, Loughrin J, McCall PJ, Röse US, Lewis WJ, Tumlinson JH. 1995. How caterpillar-damaged plants protect themselves by attracting parasitic wasps. Proc Natl Acad Sci USA. 92: 4169-4174.

Verhage A, Vlaardingerbroek I, Raaymakers C, Van Dam NM, Dicke M, Van Wees SCM, et al. 2011. Rewiring of the jasmonate signaling pathway in Arabidopsis during insect herbivory. Front Plant Sci. 2: 47. doi:10.3389/fpls.2011.00047.

Wang L, Mitra RM, Hasselmann KD, Sato M, Lenarz Wyatt L, Cohen JD, et al. 2008. The genetic network controlling the Arabidopsis transcriptional response to *Pseudomonas syringae* pv. *maculicola*: roles of major regulators and phytotoxin coronatine. Mol Plant Microbe Interact. 21: 1408-1420.

Weber H, Chételat A, Reymond P, Farmer EE. 2004. Selective and powerful stress gene expression in Arabidopsis in response to malondialdehyde. Plant J. 37: 877-888.

Whalen MC, Innes RW, Bent AF, Staskawicz BJ. 1991. Identification of *Pseudomonas syringae* pathogens of Arabidopsis and a bacterial locus determining avirulence on both Arabidopsis and soybean. Plant Cell. 3: 49-59.

Yamauchi Y, Furutera A, Seki K, Toyoda Y, Tanaka K, Sugimoto Y. 2008. Malondialdehyde generated from peroxidized linolenic acid causes protein modification in heat-stressed plants. Plant Physiol Biochem. 46: 786-793.

Yan J, Zhang C, Gu M, Bai Z, Zhang W, Qi T, et al. 2009. The Arabidopsis CORONATINE INSENSITIVE1 protein is a jasmonate receptor. Plant Cell. 21: 2220-2236.

Yan Z and Wang C. 2006. Wound-induced green leaf volatiles cause the release of acetylated derivatives and a terpenoid in maize. Phytochemistry. 67: 34–42.

Zeringue HJ. 1992. Effects of C6-C10 alkenals and alkanals on eliciting a defense response in the developing cotton boll. Phytochemistry. 31: 6-9.
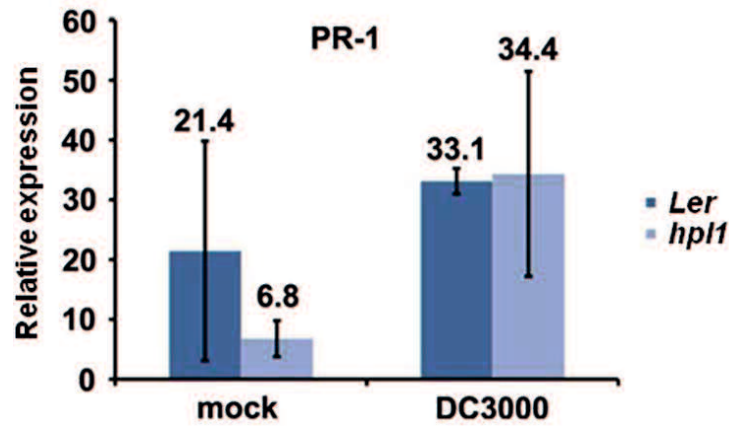
Appendix

Figure 2-8. *PR-1* expression is equally induced in *Ler* and *hpl1*. *PR-1* transcript levels were measured by qRT-PCR in *Ler* and *hpl1* infected with DC3000 48 hpi and normalized for SAND transcript levels. Error bars represent standard error.
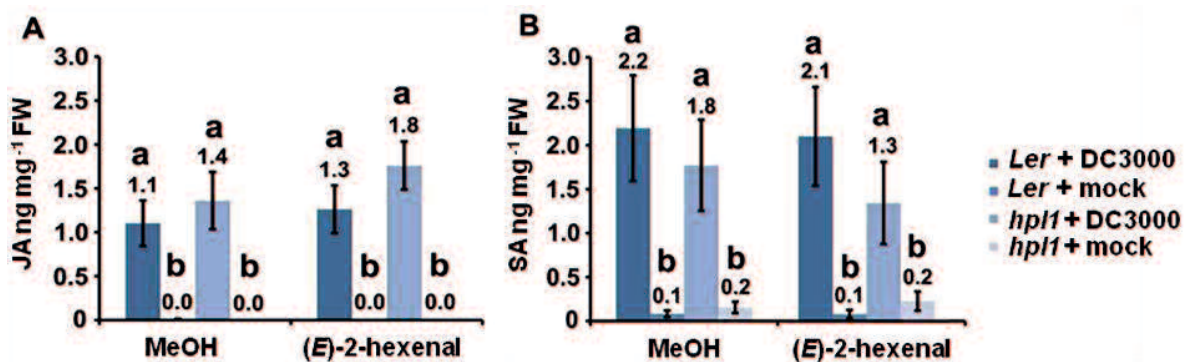
Figure 2-9. (*E*)-2-hexenal does not induce changes in JA and SA levels in *Ler* and *hpl1* plants infected with DC3000. (A) JA levels in *Ler* and *hpl1* plants pre-treated with (*E*)-2-hexenal or MeOH and subsequently infected with DC3000 (48 hpi); (B) SA levels in *Ler* and *hpl1* plants pre-treated with (*E*)-2-hexenal or MeOH and subsequently infected with DC3000 (24 hpi). In both cases the hormone levels in the 10 mM $MgSO_4$ (mock) infiltrated plants are also shown. Nine leaves were harvested, in pools of three from mock-infiltrated or bacteria-infiltrated plants at specified time points and used for plant hormone quantification. Bars represent the mean of three independent experiments. Error bars represent standard error. Bars annotated with different letters indicate statistically different hormone levels ($P < 0.05$, according to ANOVA, followed by a LSD post hoc test).

3   CHAPTER THREE

A LC-MS/MS system to analyze plant metabolites formed during stress

response

Abstract

It has been reported that reactive carbonyl species harboring α, β-unsaturated carbonyl moieties are detoxified through conjugation with glutathione (GSH).The conjugation reaction proceeds either spontaneously or enzymatically via GSH *S*-transferases. Because methacrolein (MACR) has the α, β-unsaturated carbonyl moiety, it is probable that a portion of the MACR taken up by plant tissues would be converted to its GSH adduct [S-3-(2-methylpropanal)glutathione, (MACR-GSH)] in the tissues. Tomato shoots enclosed in a jar with MACR-vapor efficiently absorbed MACR to form MACR-GSH and [S-3-(2-methylpropan-1-ol)glutathione, (MAA-GSH)]. MACR-GSH amount rapidly increases and reaches maximum level within 10 min while MAA-GSH increases from 1 min after MACR exposure and reaches maximum levels at 30 min. A sensitive analytical system is therefore crucial for the detection of GSH adducts formed in tomato plants after exposure to MACR vapor. In the first part, we established a highly sensitive LC-MS/MS system for the analysis of GSH conjugates formed in tomato tissues exposed to MACR-vapor. Thanks to this methodology, MACR-GSH and MAA-GSH peaks were detected in tomato tissues exposed to MACR vapor.

Jasmonic acid (JA) and related cyclopentanone products of the allene oxide synthase (AOS) pathway, are essential signal molecules in the defense against mechanical wounding and attacks by herbivores and necrotrophic pathogens; they are also involved in developmental processes. JA accumulates rapidly in wounded leaf and is readily detectable in the first 5 min after wounding. In the second part, a rapid sample preparation procedure and an efficient LC-MS/MS system was established to study the production of jasmonate metabolites. With this system, JA, 12-oxo-phytodienoic acid (OPDA), and jasmonic acid-isoleucine (JA-Ile) were

detected in a methanol extract of the model liverwort *Marchantia polymorpha* and algae *Klebsormidium flaccidum*.

3.1 Introduction

Plants emit vast amounts of volatile organic chemicals (VOCs) into atmosphere. A large portion of the VOCs emitted by plants are oxygenated to yield reactive carbonyl species (RCSs), which have a big impact on atmospheric chemistry. Deposition to vegetation driven by the absorption of RCSs into plants plays a major role in cleansing the atmosphere. A significant portion of the deposition to vegetation is attributable to the uptake of VOCs by plants, and a field study showed that methyl vinyl ketone (MVK) and MACR the major RCSs formed from isoprene, were immediately lost once they entered a leaf through stomata (Karl et al., 2010).

It has been reported that reactive carbonyl species harboring α, β-unsaturated carbonyl moieties are detoxified through conjugation with glutathione (GSH) (Davoine et al., 2005; Davoine et al., 2006; Mano, 2012). The conjugation reaction proceeds either spontaneously or enzymatically via GSH S-transferases (Davoine et al., 2006). Because MACR has the α, β-unsaturated carbonyl moiety, it is probable that a portion of the MACR taken up by plant tissues would be converted to its GSH adduct (MACR-GSH) in the tissues.

Tomato shoots enclosed in a jar with MACR-vapor efficiently absorbed MACR to form MACR-GSH conjugate which is formed through spontaneous conjugation between endogenous GSH and exogenous MACR, and is further reduced to form (MAA-GSH) a reduction catalyzed by an NADPH-dependent enzyme in tomato leaves (Muramoto et al., 2015). Glutathionylation was the metabolic pathway most responsible for the absorption of MACR in tomato plants (Muramoto et al., 2015). MACR-GSH and MAA-GSH are quickly formed and can be detected in tomato tissues even at 3 s to 4 s after the onset of exposure to MACR-vapor (Muramoto et al., 2015). MACR-GSH amount reaches maximum level within 10 min while MAA-GSH increases

75

from 1 min after MACR exposure and reaches maximum levels at 30 min (Muramoto et al., 2015).

Taking this into account, a sensitive analytical system is essential for the analysis of GSH conjugates formed in tomato tissues after exposure to MACR-vapor. In this first part, a highly sensitive LC-MS/MS system was established for the analysis of GSH conjugates by analyzing MACR-GSH and MAA-GSH formed in tomato tissues exposed to MACR-vapor.

JA and its related cyclopentanone products are formed from the AOS pathway. AOS (CYP74A) transforms 13-HPOT to epoxy octadecatrienoic acid (EOT), which is converted spontaneously into α- and γ-ketols, and 12-oxophytodienoic acid (OPDA). In the presence of allene oxide cyclase, EOT is specifically converted to OPDA, and then, to JA after several enzymatic reaction steps (Froehlich et al. 2001; Mosblech et al. 2009). JA can be further modified by conjugation with amino acids such as isoleucine to yield corresponding jasmonoyl derivative jasmonoyl-Ile (JA-Ile). Jasmonates are essential signal molecules in the defense against mechanical wounding and attacks by herbivores and necrotrophic pathogens; they are also involved in developmental processes (Creelman & Mullet 1997; Staswick & Lehman 1999; Brioudes et al., 2009; Glauser et al., 2009; Hause et al., 2009; Erb et al., 2012).

JA accumulates rapidly in wounded leaf and is readily detectable in the first 5 min after wounding (Glauser et al., 2008). In this second part, a rapid sample preparation procedure and an efficient LC-MS/MS system was established to study the production of jasmonate metabolites in wounded *M. polymorpha* and *K. flaccidum*. We investigated JA, OPDA, and JA-Ile in a methanol extract of the model liverwort and algae.

3.2 Materials and methods

3.2.1 Plant materials and growth conditions

Seeds of wild type tomato plants (*Solanum lycopersicum* cv. Micro-tom) obtained from the Agriculture and Forestry Research Center (Chiba, Japan) were grown under 14 h light (fluorescent lights at 60 μmol m^{-2}s^{-1})/10 h dark conditions at 25 °C on soil composed of vermiculite and Takii Tanemakibaido (Takii and Co. Ltd., Kyoto, Japan) (volume ratio of 1:1) in a plastic pot (6-cm i.d.). The tomato plants were watered every 3 d with Hyponex Concentrated Liquid (HYPONeX JAPAN Co. Ltd., Osaka, Japan) diluted to 0.1%.

M. polymorpha, Takaragaike-1 was grown on 1.4% agar with 0M51C medium at 22-25 °C under a 14 h/10 h light/dark cycle (Ishizaki et al. 2008). *K. flaccidum* strain NIES-2285 was grown at 22 °C on a 14 h/10 h light/dark cycles as described (Hori et al. 2014).

3.2.2 MACR-*vapor treatment on tomato plants*

The aerial parts of 3- to 4-week-old tomato were cut at the stem-root junction. The cut surface was covered with water-soaked cotton and then aluminum foil. The shoot was exposed to MACR (Sigma-Aldrich Co., St. Louis, MO, USA)-vapor in a 187 mL glass jar. For the treatment, 9.35 μL of MACR dissolved in 3.5% (w v^{-1}) Tween 20 at 0.5 M was impregnated in a cotton swab, and the swab was attached to the aluminum cap of the jar. The concentration of MACR in the inner space of jar would be 560 μL L^{-1}. After exposure, the leaves were harvested and snap-frozen with liquid nitrogen for further analysis.

3.2.3 Synthesis of GSH conjugates

To obtain MACR-GSH with high purity, 3.25 mmol of GSH (Wako Pure Chemical Industries, Ltd.) was mixed with an excess amount (24.2 mmol) of MACR in 20 mM borate buffer, pH10.0 and reacted for 1 h under an argon atmosphere. The reaction was stopped by adjusting the pH to 4.0 with 10% formic acid, and the surplus MACR was evaporated out with N_2 gas flow. Complete consumption of GSH was confirmed by TLC analysis on silica plates (Silica gel 60 F254, Merck KGaA, Darmstadt, Germany) using acetonitrile/water/acetic acid (80/20/0.1, v/v) as the developing solvent. The compounds were visualized with anisaldehyde or ninhydrin reagent. The product was freeze-dried and subjected to LC-MS/MS analysis. A total ion chromatogram obtained with the enhanced mass (EMS) mode indicated >90% purity of MACR-GSH. MAA-GSH was synthesized by adding an excess amount of $NaBH_4$ to MACR-GSH in 20 mM borate buffer, pH 10.0. Identification of the compounds was performed by LC-MS/MS with EMS mode (**Figure 3-3**) using a LC-MS/MS [3200 Q-TRAP LC/MS/MS System (AB Sciex, Framingham, MA, USA) equipped with a Prominence UFLC (Shimadzu, Kyoto, Japan)]. The products were separated on a Mightysil RP18 column (150-mm × 2-mm i.d.) with a binary gradient consisting of water:formic acid (100:0.1, v/v, solvent A) and acetonitrile:formic acid (100:0.1, v/v, solvent B). The run consisted of 100% A for 5 min, a linear increase from 100% A to 100% B over 25 min (flow rate, 0.2 mL min^{-1}), and 100% B for 2 min. Compounds were detected by MS/MS using electro-spray ionization in the positive ion mode [ion spray voltage: 5000 V, nitrogen as both the curtain gas (set to 20 arbitrary units) and collision gas (set to 'high'), collision energy: 19 V, scan range: *m/z* 100 to 1200, scan speed: 4,000 Da s^{-1}, declustering potential: 26 V].

3.2.4   *Analysis of GSH adducts in tomato leaves*

The frozen powder prepared from tomato leaves (80 mg) was suspended in 1 mL of 20 mM borate buffer, pH 4.0 containing 5 µg of *S*-hexylglutathione (Hex-GSH) (Sigma-Aldrich Co.) as an IS. The GSH-adducts were extracted with a beads cell disruptor for 1 min at 3500 rpm. The suspension was centrifuged at 8000 g for 15 min at 4 °C. The supernatant was filtered through an Ekicrodisc 3 (HPLC Certified, 0.45 µm, 3 mm; Pall Corporation, Port Washington, NY). GSH conjugates in the extract were scanned by analysis in the EMS mode as shown above or in the neutral loss mode, which permitted the determination of the *m/z* ratio of pseudomolecular ions undergoing neutral loss of 75 mass units (part of glycine) upon fragmentation of the compounds under the same MS conditions used in EMS mode. The compounds were identified by comparing the mass spectra (obtained with EMS mode) and their retention times with those of standard compounds. For quantification of GSH conjugates in the sample, LC-MS/MS analysis in the multiple reaction monitoring (MRM) mode was performed. The parameters used for MRM detection are shown in **Table 3-1**.

3.2.5   *Analysis of OPDA, JA, and JA-Ile in* **Marchantia** *and* **Klebsormidium** *spp*

OPDA, JA, and JA-Ile were extracted from triplicate samples of *M. polymorpha* and *K. flaccidum* as described (Wu et al. 2007). Approximately 150 mg of *M. polymorpha* thallus was collected in a screw-cap tube containing zirconia beads, frozen in liquid nitrogen, and homogenized with a mini bead-beater (Waken BTech. Kyoto, Japan). Ethyl acetate (0.5 mL) spiked with 200 ng D_2JA, the internal standard, was added to each sample and then homogenized again with the mini bead-beater. The *K. flaccidum* cells were also homogenized with mortar and pestle under liquid nitrogen, and then extracted as described above. After centrifugation at

13,000 × *g* for 20 min at 4 °C, supernatants were transferred to fresh 1.5 mL Eppendorf tubes. Each pellet was re-extracted with 0.5 mL ethyl acetate and centrifuged at the same speed as mentioned above; supernatants were combined and evaporated to dryness on a vacuum concentrator (TAITEC). The dried residues were resuspended with 0.5 mL of 70% methanol (v/v) and analyzed by LC-MS/MS.

JA and JA-Ile were analyzed by LC-MS/MS (3200 Q-TRAP LC/MS/MS System, ABSciex, Framingham, MA) equipped with Prominence UFLC (Shimadzu, Kyoto, Japan). At a flow rate of 0.2 mL min^{-1}, 2 μL of each sample was injected onto a Mightysil RP18 column (5 μm, 150 × 2 mm). A mobile phase composed of solvent A [water/acetonitrile/formic acid (90:10:0.1, v/v)] and solvent B [acetonitrile/water/formic acid (95:5:0.1, v/v)] was used in a gradient mode for separation. The solvent gradient was 100% A to 100% B over 20 min, followed by a 5 min hold at 100% B. The MS was used in negative ion mode and ions were detected using Multiple Reaction Monitoring. Quantification was based on the internal standard and standard curves (Mwenda et al. 2015; Koeduka et al. 2015).

3.3 Results

3.3.1 *Glutathionylation*

It has been reported that reactive carbonyl species harboring α,β-unsaturated carbonyl moieties are detoxified through conjugation with glutathione (GSH) (Davoine et al., 2005; Davoine et al., 2006; Mano, 2012). The conjugation reaction proceeds either spontaneously or enzymatically via GST (Davoine et al., 2006). Because MACR has the α,β-unsaturated carbonyl moiety, we assumed that a portion of the MACR taken up by tomato plants would be converted to its GSH adduct [*S*-3-(2-methylpropanal)glutathione, MACR-GSH] in the tissues. To examine

the formation of the conjugate, we first synthesized MACR-GSH, and established an analytical system with LC-MS/MS (**Figures 3-1 and 3-2**). When an extract prepared from tomato plants exposed to MACR-vapor at 560 μL L^{-1} in a glass jar (187 mL) for 2 h was subjected to LC-MS/MS analysis, we detected a peak corresponding to MACR–GSH. At the same time, a big peak with an *m/z* of 380 was detected. This peak coincided with the compound prepared from synthetic MACR–GSH through reduction with $NaBH_4$; thus, it was assigned as the GSH adduct of MAA [*S*-3-(2-methylpropan-1-ol) glutathione (MAA-GSH)]. The MS profiles of synthetic MAA-GSH and the compound detected in the MACR-exposed tomato tissues supported this assignment (**Figure 3-2**). When the extract was analyzed in the neutral loss mode (−75 Da; corresponding to the removal of glycine with the aim of detecting all GSH adducts, only peaks corresponding to MACR-GSH and MAA-GSH were detected (**Figure 3-3**).
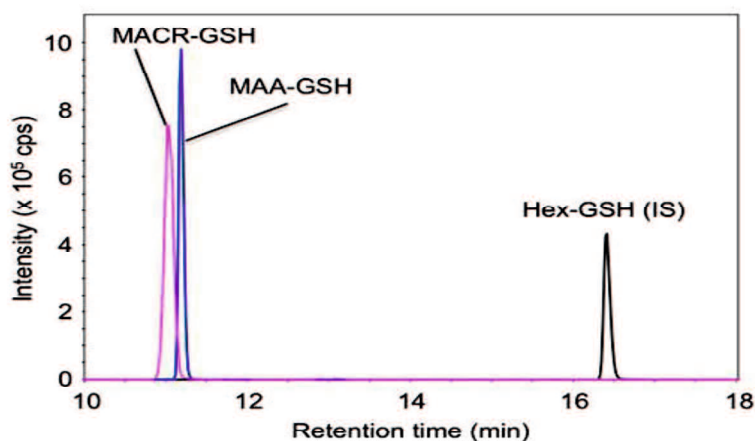

Figure 3-1. A representative chromatograph of a mixture of synthetic MACR-GSH, MAA-GSH, and Hex-GSH (included as internal standard) obtained with MRM mode of LC-MS/MS
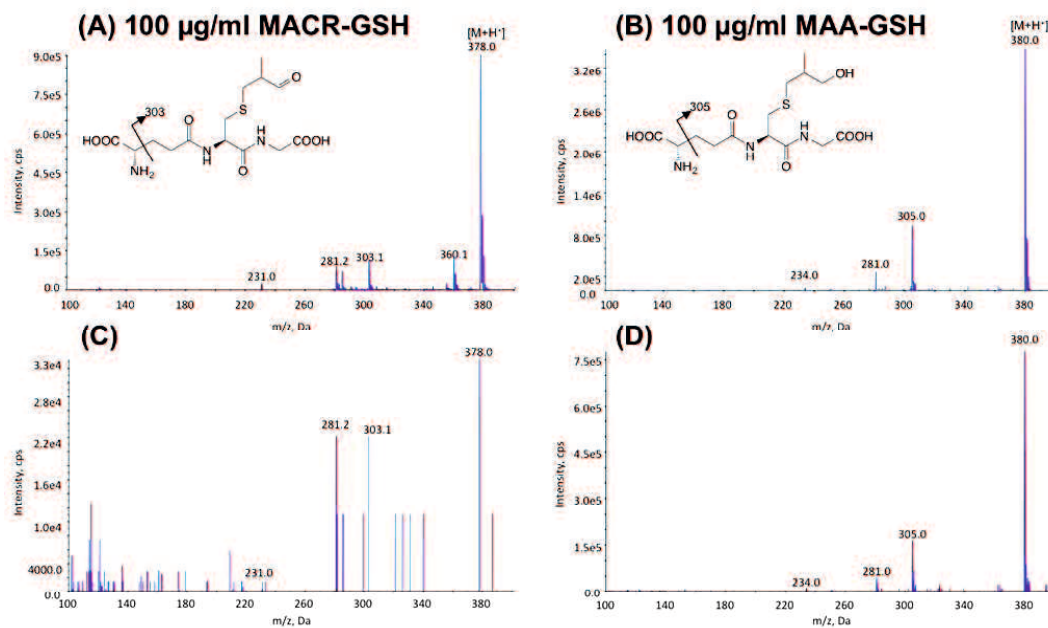
Figure 3-2. MS profile of synthesized MACR-GSH (A) and MAA-GSH (B) and the corresponding peaks (C and D) detected in tomato tissues exposed to 560 μL L^{-1} MACR-vapor for 2 h. LC-MS/MS analysis was performed with the enhanced MS mode
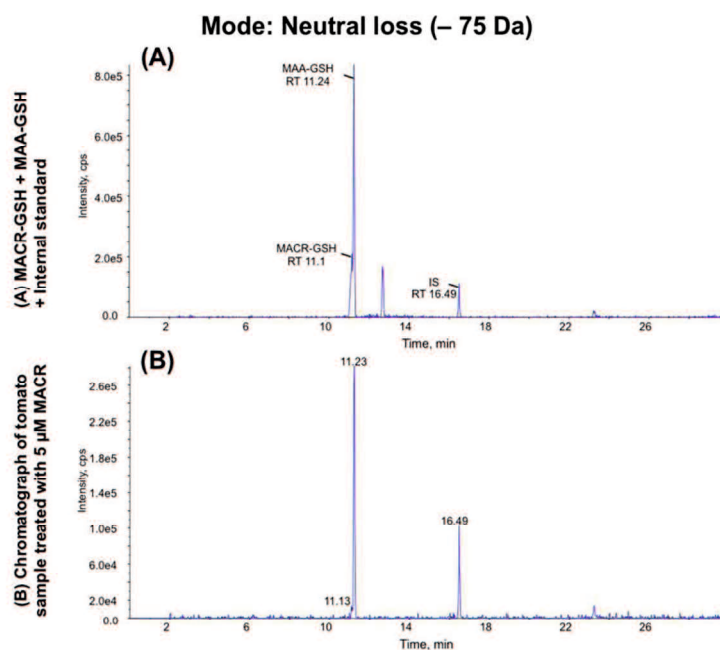

Figure 3-3. Chromatograph obtained with the neutral loss mode (-75 Da) of LC-MS/MS to examine GSH conjugates formed in tomato leaves after exposure to MACR. (A) Chromatograph of authentic standards (B) Chromatograph of extract obtained from tomato sample with 560 μL L^{-1} MACR for 2 h.

Table 3-1. Parameters used for MRM analysis of GSH conjugates

	Q1 (Da)	Q3 (Da)	Dwell (msec)	CEP (V)	CE (V)
MACR-GSH	378.133	231.100	200	18.00	19.00
MAA-GSH	380.000	234.000	200	22.35	21.00
Hex-GSH	392.179	246.100	200	22.82	21.00

3.3.2 *Analysis of endogenous OPDA, JA, and JA-Ile in* Marchantia *and* Klebsormidium *spp*

Jasmonates including OPDA and JA are stress response signaling molecules in angiosperms. The function of jasmonates remains unknown in the model liverwort and algae; we investigated OPDA, JA, and JA-Ile in a methanol extract of *M. polymorpha* and *K. flaccidum* by LC-MS/MS. The results showed a substantial amount of OPDA (288.8 ± 64.6 ng·g FW^{-1}) in intact *M. polymorpha* thallus, while no significant accumulation of JA and JA-Ile was observed even though the thalli were wounded (Koeduka et al., 2015). The high levels of OPDA accumulation (9.6 ± 0.6 μg·mg protein^{-1}), in contrast to JA and JA-Ile, were also found in *K. flaccidum* (Koeduka et al., 2015). The accumulation patterns of OPDA are consistent with a previous observation that *P. patens* produces mostly OPDA but not JA and JA-Ile (Scholz et al. 2012).
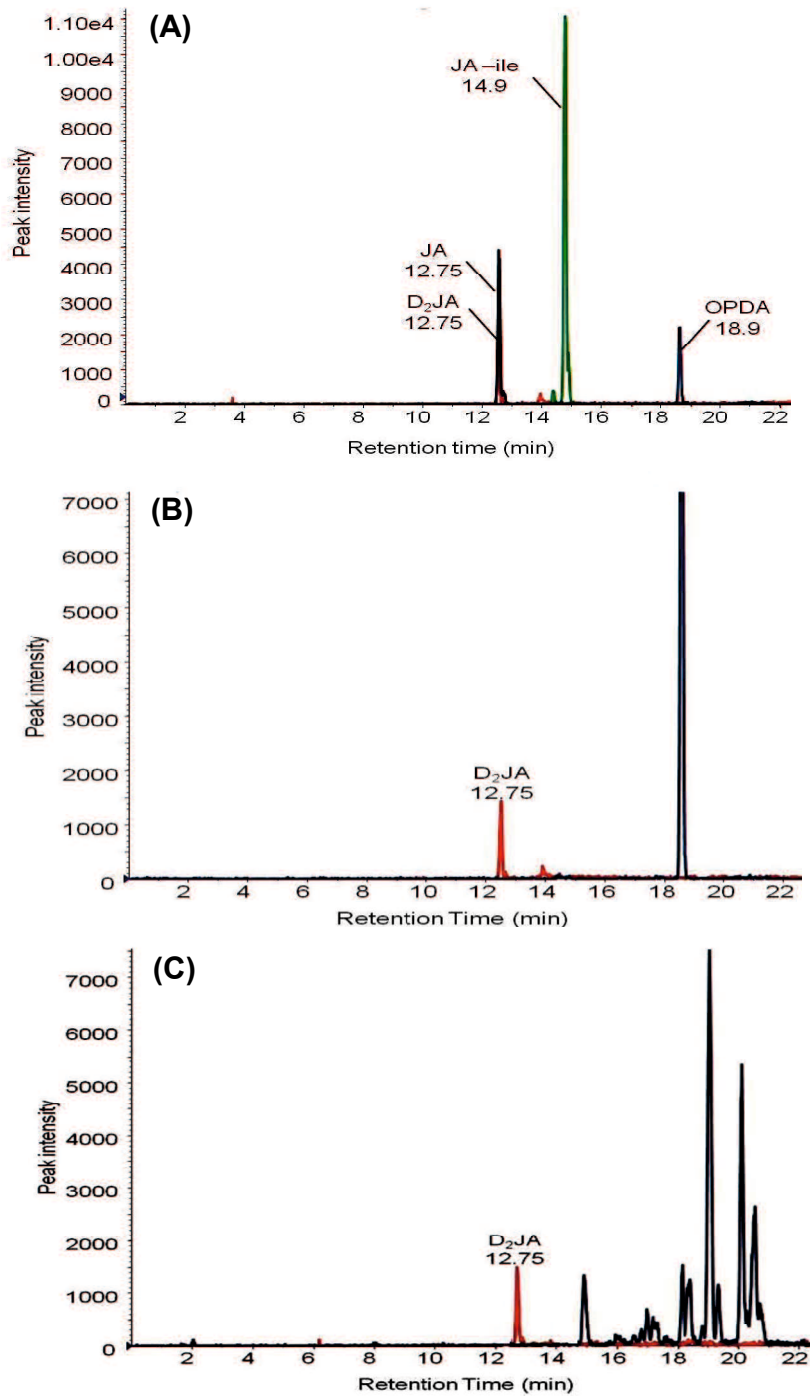
Figure 3-4. Total ion chromatograph with LC-MS/MS of standard compounds (A) and jasmonates in wounded *M. polymorpha* (B) and *K. flaccidum* (C).Magenta chromatogram D_2JA (IS), black JA, green (JA-Ile) and blue (OPDA)

3.4 Discussion

It has been reported that reactive carbonyl species harboring α,β-unsaturated carbonyl moieties are detoxified through conjugation with glutathione (GSH) (Davoine et al., 2005; Davoine et al., 2006; Mano, 2012). The conjugation reaction proceeds either spontaneously or enzymatically via GST (Davoine et al., 2006). Because MACR has the α,β-unsaturated carbonyl moiety, it is assumed that a portion of the MACR taken up by tomato plants would be converted to its GSH adduct [*S*-3-(2-methylpropanal)glutathione, MACR-GSH] in the tissues (Muramoto et al., 2015). The established LC-MS/MS analysis system enabled us to detect peaks of MACR-GSH and MAA-GSH conjugates formed in tomato tissues exposed to MACR-vapor at 560 µL L^{-1} in a glass jar (187 mL) for 2 h. Hence, this system can be used for the quantification and detection of all GSH adducts formed in tomato plants exposed to MACR-vapor. Probably, GSH-conjugates formed in other plant tissues can be detected using this system.

In angiosperms, OPDA and JA are independently responsible for the defense response to biotic and abiotic stresses (Taki et al. 2005; Scalschi et al. 2015). In this second part, incorporation of a rapid sample preparation procedure and LC-MS/MS analysis enabled the detection of jasmonates. The metabolite analysis of *M. polymorpha* and *K. flaccidum* showed substantial levels of OPDA but no accumulation of JA and JA-Ile, unlike Arabidopsis and other organisms (Koeduka et al., 2015; Mwenda et al. 2015). A similar result was obtained by Yamamoto et al. 2015. This system can be used for jasmonate analysis with other plant tissues (Mwenda et al. 2015).

3.5 References

Brioudes F, Joly C, Szécsi J. 2009. Jasmonates control late development stages of petal growth in *Arabidopsis thaliana*. Plant J. 60, 1070-1080.

Creelman RA, Mullet JE. 1997. Biosynthesis and action of jasmonates in plants. Annu Rev Plant Physiol Mol Biol. 48: 355-381.

Davoine C, DT. 2005. Conjugation of keto fatty acids to glutathione in plant tissues. Characterization and quantification by HPLC-tandem mass spectrometry. Anal Chem. 77: 7366-7372.

Davoine C, Falletti O, Douki T, Iacazio G, Ennar N, Montillet JL, Triantaphylidés C. 2006. Adducts of oxylipin electrophiles to glutathione reflect a 13 specificity of the down stream lipoxygenase pathway in the tobacco hypersensitive response. Plant Physiol 140: 1484-1493.

Erb M, Meldau S, Howe GA. 2012. Role of phytohormones in insect-specific plant reactions. Trends in Plant Science. 17: 250-259.

Froehlich JE, Itoh A, Howe GA. 2001. Tomato allene oxide synthase and fatty acid hydroperoxide lyase, two cytochrome P450s involved in oxylipin metabolism, are targeted to different membranes of chloroplast envelope. Plant Physiol. 125: 306-317.

Glauser G, Dubugnon L, Mousavi SA, Rudaz S, Wolfender J-L, Farmer EE. 2009. Velocity estimates for signal propagation leading to systemic jasmonic acid accumulation in wounded Arabidopsis. J Biol Chem. 284. 34506-34513.

Glauser G, Grata E, Dubugnon L, Rudaz S, Farmer EE, Wolfender J-L. 2008. Spatial and temporal dynamics of jasmonate synthesis and accumulation in Arabidopsis in response to wounding. Journal of Biological Chemistry. 283: 16400-16407.

Hause B, Wasternack C, Strack D. 2009. Jasmonates in stress responses and development. Phytochemistry. 70: 1483-1484.

Hori K, Maruyama F, Fujisawa T, Togashi T, Yamamoto N, Seo M, Sato S, Yamada T, Mori H, Tajima N, Moriyama T, Ikeuchi M, Watanabe M, Wada H, Kobayashi K, Saito M, Masuda T, Sasaki-Sekimoto Y, Mashiguchi K, Awai K, Shimojima M, Masuda S, Iwai M, Nobusawa T, Narise T, Kondo S, Saito H, Sato R, Murakawa M, Ihara Y, Oshima-Yamada Y, Ohtaka K, Satoh M, Sonobe K, Ishii M, Ohtani R, Kanamori-Sato M, Honoki R, Miyazaki D, Mochizuki H, Umetsu J, Higashi K, Shibata D, Kamiya Y, Sato N, Nakamura Y, Tabata S, Ida S, Kurokawa K, Ohta H. 2014. Klebsormidium flaccidum genome reveals primary factors for plant terrestrial adaptation. Nat Commun. 5: 3978.

Ishizaki K, Chiyoda S, Yamato KT, Kohchi T. 2008. Agrobacterium-mediated transformation of the haploid liverwort Marchantia polymorpha L., an emerging model for plant biology. Plant Cell Physiol. 49: 1084-1091.

Mano J. 2012. Reactive carbonyl species: Their production from lipid peroxides, action in environmental stress, and the detoxification mechanism. Plant Physiol Biochem. 59: 90-97.

Karl T, Harkey P, Emmons L, Thornton B, Guenther A, Basu C, Turnipseed A, Jardine K. 2010. Efficient atmospheric cleansing of oxidized organic trace gases by vegetation. Science. 330: 816-819.

Koeduka T, Ishizaki K, Mwenda CM, Hori K, Sasaki-Sekimoto Y, Ohta H, Kohchi T, Matsui K. 2015. Biochemical characterization of allene oxide synthases from liverwort *Marchantia polymorpha* and green micralgae *Klebsormidium flaccidum* provides insight into the evolutionary divergence of the plant CYP74 family. Planta. 242(5): 1175-1186.

Mosblech A, Thurow C, Gatz C, Feussner I, Heilmann I. 2011. Jasmonic acid perception by

    COI1 involves inositol polyphosphates in *Arabidopsis thaliana*. Plant J. 65: 949–957.

Muramoto S, Matsubara Y, Mwenda CM, Koeduka T, Sakami T, Tani A, Matsui K. 2015.

    Glutathionylation and reduction of methacrolein in tomato plants account for its

    absorption from the vapor phase. Plant Physiol. doi: 10.1104/pp.15.01045.

Mwenda CM, Matsuki A, Nishimura K, Koeduka T, Matsui K. 2015. Spatial expression of the

    Arabidopsis *hydroperoxide lyase* gene is controlled differently from that of *allene oxide*

    synthase gene. J Plant Interact. 1: 1-10.

Scalschi L, Sanmartín M, Camañes G, Troncho P, Sánchez-Serrano JJ, García-Augustin P, Vicedo

    B. 2015. Silencing of OPR3 in tomato reveals the role of OPDA in callose deposition

    during the activation of defense responses against *Botrytis cinerea*. Plant J. 81: 304-315.

Scholz J, Brodhun F, Hornung E, Herrfurth C, Stumpe M, Beike AK, Faltin B, Frank W, Reski R,

    Feussner I. 2012. Biosynthesis of allene oxides in Physcomitrella patens. BMC Plant

    Biol. 12: 228.

Staswick PE, Lehman CC. 1999. Jasmonic acid-signalled responses in plants. In: Agrawal AA,

    Tazun S, Bent E, editor. Induced plant defenses against pathogens and herbivores. St.

    Paul (MN). American Phytopathological Society Press: p. 117-136.

Taki N, Sasaki-Sekimoto Y, Obayashi T, Kikuta A, Kobayashi K, Ainai T, Yagi K, Sakurai N,

    Suzuki H, Masuda T, Takamiya K, Shibata D, Kobayashi Y, Ohta H. 2005. 12-oxo-

    phytodienoic acid triggers expression of a distinct set of genes and plays a rolein wound-

    induced gene expression in Arabidopsis. Plant Physiol. 139: 1268-1283.

Wu J, Hettenhausen C, Meldau S, Baldwin IT. 2007. Herbivory rapidly activates MAPK

signalling in attacked and unattacked leaf regions but not between leaves of *Nicotiana attenuata*. Plant Cell. 19: 1096-1122.

List of publications

Cynthia Mugo Mwenda, Atsushi Matsuki, Kohji Nishimura, Takao Koeduka & Kenji Matsui. 2015. Spatial expression of the Arabidopsis *hydroperoxide lyase* gene is controlled differently from that of the *allene oxide synthase* gene. J Plant Interact. 10(1): 1-10. doi: 10.1080/17429145.2014.999836

Cynthia Mugo Mwenda, Kenji Matsui. 2014. The importance of lipoxygenase control in the production of green leaf volatiles by lipase-dependent and independent pathways. Plant Biotechnology. 31: 445–452. doi: 10.5511/plantbiotechnology.14.0924a

Alessandra Scala, Rossana Mirabella, **Cynthia Mugo**, Kenji Matsui, Michel A. Haring and Robert C. Schuurink. (2013). (*E*)-2-hexenal promotes susceptibility to *Pseudomonas syringae* by activating jasmonic acid pathways in *Arabidopsis*. Frontiers in Plant Science. 4:74. doi: 10.3389/fpls.2013.00074.

Takao Koeduka, Kimitsune Ishizaki, **Cynthia Mugo Mwenda**, Koichi Hori, Yuko Sasaki-Sekimoto, Hiroyuki Ohta, Takayuki Kohchi, Kenji Matsui. 2015. Biochemical characterization of allene oxide synthases from the liverwort Marchantia polymorpha and green microalgae Klebsormidium flaccidum provides insight into the evolutionary divergence of the plant CYP74 family. Planta. 242(5):1175-1186. doi.1007/s00425-015-2355-8.

Shoko Muramoto, Yayoi Matsubara, **Cynthia Mugo Mwenda**, Takao Koeduka, Takuya Sakami, Akira Tani, Kenji Matsui. 2015. Glutathionylation and reduction of methacrolein in tomato plants account for its absorption from the vapor phase. Plant Physiol. doi:10.1104/pp.15.01045

Mugo Cynthia Nyambura, Kenji Matsui, and Toshihiro Kumamaru. 2011. Establishment of an efficient screening system to isolate rice mutants deficient in green leaf volatile formation. J Plant Interact. 6(2-3): 185-186. doi: 10.1080/17429145.2010.544777.

Academic presentations

<u>2012</u>

Cynthia Mugo Mwenda, Alessandra Scala, 松井健二、高林純示、Robert C. Schuurink (2012) Deficiency in green leaf volatiles attenuates Arabidopsis early response against *Pseudomonas syringae*. Talk presented at JSPS Core-to-Core Program Symposium, 2012年10月15-16日 Max Plank Institute of Chemical Ecology, Jena, Germany

Cynthia Mugo Mwenda, Alessandra Scala, 松井健二、高林純示、Robert C. Schuurink (2012) Deficiency in green leaf volatiles attenuates Arabidopsis early response against *Pseudomonas syringae*. 日本農芸化学会中四国支部大会（第34回講演会）　2012年9月21-22日 山口大学工学部

<u>2013</u>

Cynthia Mugo Mwenda, Atsushi Matsuki, and Kenji Matsui (2013) Spatiotemporal expression of hydroperoxide lyase gene in Arabidopsis.
日本農芸化学会関西・中四国・西日本支部2013年度合同広島大会　2013年9月5-6日
県立広島大学広島キャンパス（口頭発表）

Cynthia Mugo, Atsushi Matsuki, and Kenji Matsui (2013) Spatiotemporal expression of hydroperoxide lyase gene in Arabidopsis -its fine control distinct from that of allene oxide synthase gene-. Poster presented at 2013 Annual Meeting of the Korean Society of Plant Biologists & the 5th Asian Symposium on Plant Lipids, 2013年11-12月29-1日 Gwangju, Korea